7 Magnetic surveying

7.1 Introduction

The aim of a magnetic survey is to investigate subsurface geology on the basis of anomalies in the Earth's magnetic field resulting from the magnetic properties of the underlying rocks. Although most rock-forming minerals are effectively non-magnetic, certain rock types contain sufficient magnetic minerals to produce significant magnetic anomalies. Similarly, man-made ferrous objects also generate magnetic anomalies. Magnetic surveying thus has a broad range of applications, from small-scale engineering or archaeological surveys to detect buried metallic objects, to large-scale surveys carried out to investigate regional geological structure.

Magnetic surveys can be performed on land, at sea and in the air. Consequently, the technique is widely employed, and the speed of operation of airborne surveys makes the method very attractive in the search for types of ore deposit that contain magnetic minerals.

7.2 Basic concepts

Within the vicinity of a bar magnet a magnetic flux is developed which flows from one end of the magnet to the other (Fig. 7.1). This flux can be mapped from the directions assumed by a small compass needle suspended within it. The points within the magnet where the flux converges are known as the poles of the magnet. A freely-suspended bar magnet similarly aligns in the flux of the Earth's magnetic field. The pole of the magnet which tends to point in the direction of the Earth's north pole is called the north-seeking or positive pole, and this is balanced by a south-seeking or negative pole of identical strength at the opposite end of the magnet.

The force F between two magnetic poles of strengths m_1 and m_2 separated by a distance r is given by

$$F = \frac{\mu_0 m_1 m_2}{4\pi\mu_R r^2} \tag{7.1}$$

where μ_0 and μ_R are constants corresponding to the *magnetic permeability of vacuum* and the *relative magnetic permeability* of the medium separating the poles (see later). The force is attractive if the poles are of different sign and repulsive if they are of like sign.

The *magnetic field B* due to a pole of strength m at a distance r from the pole is defined as the force exerted on a unit positive pole at that point

$$B = \frac{\mu_0 m}{4\pi\mu_R r^2} \tag{7.2}$$

Magnetic fields can be defined in terms of *magnetic potentials* in a similar manner to gravitational fields. For a single pole of strength m, the magnetic potential V at a distance r from the pole is given by

$$V = \frac{\mu_0 m}{4\pi\mu_R r} \tag{7.3}$$

The magnetic field component in any direction is then given by the partial derivative of the potential in that direction.

In the SI system of units, magnetic parameters are defined in terms of the flow of electrical current (see e.g. Reilly 1972). If a current is passed through a coil consisting of several turns of wire, a *magnetic flux* flows through and around the coil annulus which arises from a *magnetizing force H*. The magnitude of H is proportional to the number of turns in the coil and the strength of the current, and inversely proportional to the length of the wire, so that H is expressed in A m^{-1}. The density of the magnetic flux, measured over an area perpendicular to the direction of flow, is known as the *magnetic induction* or *magnetic field B* of the coil. B is proportional to H and the constant of proportionality μ is known as the *magnetic permeability*. Lenz's law of induction relates the rate of change of magnetic flux in a circuit to the voltage devel-

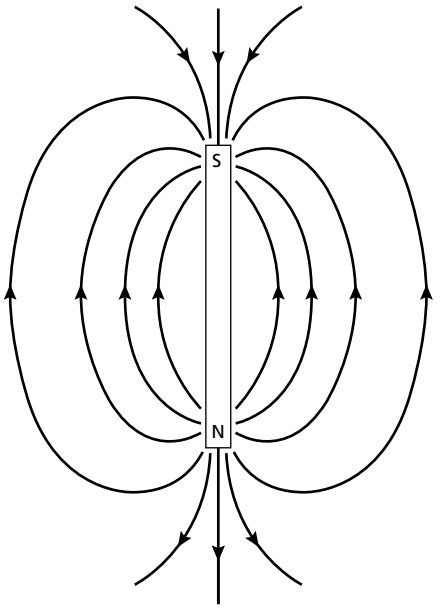

Fig. 7.1 The magnetic flux surrounding a bar magnet.

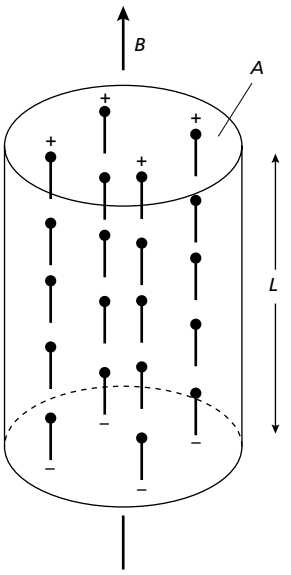

Fig. 7.2 Schematic representation of an element of material in which elementary dipoles align in the direction of an external field B to produce an overall induced magnetization.

oped within it, so that B is expressed in $\mathrm{Vs\,m^{-2}}$ (Weber (Wb) $\mathrm{m^{-2}}$). The unit of the $\mathrm{Wb\,m^{-2}}$ is designated the *tesla* (T). Permeability is consequently expressed in $\mathrm{Wb\,A^{-1}\,m^{-1}}$ or Henry (H) $\mathrm{m^{-1}}$. The c.g.s. unit of magnetic field strength is the *gauss* (G), numerically equivalent to 10^{-4} T.

The tesla is too large a unit in which to express the small magnetic anomalies caused by rocks, and a subunit, the *nanotesla* (nT), is employed ($1\,\mathrm{nT} = 10^{-9}\,\mathrm{T}$). The c.g.s. system employs the numerically equivalent *gamma* (γ), equal to 10^{-5} G.

Common magnets exhibit a pair of poles and are therefore referred to as dipoles. The *magnetic moment* M of a dipole with poles of strength m a distance l apart is given by

$$M = ml \tag{7.4}$$

The magnetic moment of a current-carrying coil is proportional to the number of turns in the coil, its cross-sectional area and the magnitude of the current, so that magnetic moment is expressed in $\mathrm{A\,m^2}$.

When a material is placed in a magnetic field it may acquire a magnetization in the direction of the field which is lost when the material is removed from the field. This phenomenon is referred to as *induced magnetization* or *magnetic polarization*, and results from the alignment of elementary dipoles (see below) within the material in the direction of the field. As a result of this alignment the material has magnetic poles distributed over its surface which correspond to the ends of the dipoles (Fig. 7.2). The intensity of induced magnetization J_i of a material is defined as the dipole moment per unit volume of material:

$$J_\mathrm{i} = \frac{M}{LA} \tag{7.5}$$

where M is the magnetic moment of a sample of length L and cross-sectional area A. J_i is consequently expressed in $\mathrm{A\,m^{-1}}$. In the c.g.s. system intensity of magnetization is expressed in emu $\mathrm{cm^{-3}}$ (emu = electromagnetic unit), where $1\ \mathrm{emu\,cm^{-3}} = 1000\ \mathrm{A\,m^{-1}}$.

The induced intensity of magnetization is proportional to the strength of the magnetizing force H of the inducing field:

$$J_\mathrm{i} = kH \tag{7.6}$$

where k is the *magnetic susceptibility* of the material. Since J_i and H are both measured in $\mathrm{A\,m^{-1}}$, susceptibility is dimensionless in the SI system. In the c.g.s. system susceptibility is similarly dimensionless, but a consequence of

rationalizing the SI system is that SI susceptibility values are a factor 4π greater than corresponding c.g.s. values.

In a vacuum the magnetic field strength B and magnetizing force H are related by $B = \mu_0 H$ where μ_0 is the permeability of vacuum ($4\pi \times 10^{-7}\,\mathrm{H\,m^{-1}}$). Air and water have very similar permeabilities to μ_0 and so this relationship can be taken to represent the Earth's magnetic field when it is undisturbed by magnetic materials. When a magnetic material is placed in this field, the resulting magnetization gives rise to an additional magnetic field in the region occupied by the material, whose strength is given by $\mu_0 J_i$. Within the body the total magnetic field, or magnetic induction, B is given by

$$B = \mu_0 H + \mu_0 J_i$$

Substituting equation (7.6)

$$B = \mu_0 H + \mu_0 kH = (1 + k)\mu_0 H = \mu_R \mu_0 H$$

where μ_R is a dimensionless constant known as the *relative magnetic permeability*. The magnetic permeability μ is thus equal to the product of the relative permeability and the permeability of vacuum, and has the same dimensions as μ_0. For air and water μ_R is thus close to unity.

All substances are magnetic at an atomic scale. Each atom acts as a dipole due to both the spin of its electrons and the orbital path of the electrons around the nucleus. Quantum theory allows two electrons to exist in the same state (or electron shell) provided that their spins are in opposite directions. Two such electrons are called paired electrons and their spin magnetic moments cancel. In *diamagnetic* materials all electron shells are full and no unpaired electrons exist. When placed in a magnetic field the orbital paths of the electrons rotate so as to produce a magnetic field in opposition to the applied field. Consequently, the susceptibility of diamagnetic substances is weak and negative. In *paramagnetic* substances the electron shells are incomplete so that a magnetic field results from the spin of their unpaired electrons. When placed in an external magnetic field the dipoles corresponding to the unpaired electron spins rotate to produce a field in the same sense as the applied field so that the susceptibility is positive. This is still, however, a relatively weak effect.

In small grains of certain paramagnetic substances whose atoms contain several unpaired electrons, the dipoles associated with the spins of the unpaired electrons are magnetically coupled between adjacent atoms. Such a grain is then said to constitute a single *magnetic domain*. Depending on the degree of overlap of the electron orbits, this coupling may be either parallel or antiparallel. In *ferromagnetic* materials the dipoles are parallel (Fig. 7.3), giving rise to a very strong spontaneous magnetization which can exist even in the absence of an external magnetic field, and a very high susceptibility. Ferromagnetic substances include iron, cobalt and nickel, and rarely occur naturally in the Earth's crust. In *antiferromagnetic* materials such as haematite, the dipole coupling is antiparallel with equal numbers of dipoles in each direction. The magnetic fields of the dipoles are self-cancelling so that there is no external magnetic effect. However, defects in the crystal lattice structure of an antiferromagnetic material may give rise to a small net magnetization, called *parasitic antiferromagnetism*. In *ferrimagnetic* materials such as magnetite, the dipole coupling is similarly antiparallel, but the strength of dipoles in each direction are unequal. Consequently ferrimagnetic materials can exhibit a strong spontaneous magnetization and a high susceptibility. Virtually all the minerals responsible for the magnetic properties of common rock types (Section 7.3) fall into this category.

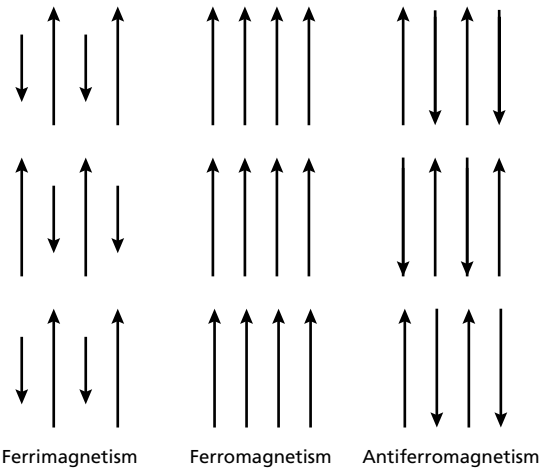

Fig. 7.3 Schematic representation of the strength and orientation of elementary dipoles within ferrimagnetic, ferromagnetic and antiferromagnetic domains.

The strength of the magnetization of ferromagnetic and ferrimagnetic substances decreases with temperature and disappears at the *Curie temperature*. Above this temperature interatomic distances are increased to separations which preclude electron coupling, and the material behaves as an ordinary paramagnetic substance.

In larger grains, the total magnetic energy is decreased if the magnetization of each grain subdivides into individual volume elements (magnetic domains) with diameters of the order of a micrometre, within which there is parallel coupling of dipoles. In the absence of any external magnetic field the domains become oriented in such a way as to reduce the magnetic forces between adjacent domains. The boundary between two domains, the *Bloch wall*, is a narrow zone in which the dipoles cant over from one domain direction to the other.

When a multidomain grain is placed in a weak external magnetic field, the Bloch wall unrolls and causes a growth of those domains magnetized in the direction of the field at the expense of domains magnetized in other directions. This induced magnetization is lost when the applied field is removed as the domain walls rotate back to their original configuration. When stronger fields are applied, domain walls unroll irreversibly across small imperfections in the grain so that those domains magnetized in the direction of the field are permanently enlarged. The inherited magnetization remaining after removal of the applied field is known as *remanent*, or *permanent*, *magnetization* J_r. The application of even stronger magnetic fields causes all possible domain wall movements to occur and the material is then said to be magnetically saturated.

Primary remanent magnetization may be acquired either as an igneous rock solidifies and cools through the Curie temperature of its magnetic minerals (thermoremanent magnetization, TRM) or as the magnetic particles of a sediment align within the Earth's field during sedimentation (detrital remanent magnetization, DRM). Secondary remanent magnetizations may be impressed later in the history of a rock as magnetic minerals recrystallize or grow during diagenesis or metamorphism (chemical remanent magnetization, CRM). Remanent magnetization may develop slowly in a rock standing in an ambient magnetic field as the domain magnetizations relax into the direction of the field (viscous remanent magnetization, VRM).

Any rock containing magnetic minerals may possess both induced and remanent magnetizations J_i and J_r. The relative intensities of induced and remanent magnetizations are commonly expressed in terms of the *Königsberger ratio*, $J_r : J_i$. These may be in different directions and may differ significantly in magnitude. The magnetic effects of such a rock arise from the resultant J of the two magnetization vectors (Fig. 7.4). The magnitude of J controls the amplitude of the magnetic anomaly and the orientation of J influences its shape.

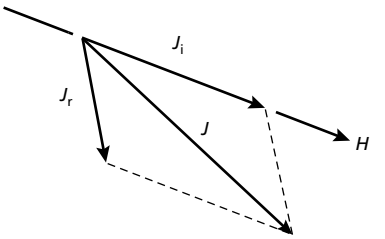

Fig. 7.4 Vector diagram illustrating the relationship between induced (J_i), remanent (J_r) and total (J) magnetization components.

7.3 Rock magnetism

Most common rock-forming minerals exhibit a very low magnetic susceptibility and rocks owe their magnetic character to the generally small proportion of magnetic minerals that they contain. There are only two geochemical groups which provide such minerals. The iron–titanium–oxygen group possesses a solid solution series of magnetic minerals from magnetite (Fe_3O_4) to ulvöspinel (Fe_2TiO_4). The other common iron oxide, haematite (Fe_2O_3), is antiferromagnetic and thus does not give rise to magnetic anomalies (see Section 7.12) unless a parasitic antiferromagnetism is developed. The iron–sulphur group provides the magnetic mineral pyrrhotite (FeS_{1+x}, $0 < x < 0.15$) whose magnetic susceptibility is dependent upon the actual composition.

By far the most common magnetic mineral is magnetite, which has a Curie temperature of 578°C. Although the size, shape and dispersion of the magnetite grains within a rock affect its magnetic character, it is reasonable to classify the magnetic behaviour of rocks according to their overall magnetite content. A histogram illustrating the susceptibilities of common rock types is presented in Fig. 7.5.

Basic igneous rocks are usually highly magnetic due to their relatively high magnetite content. The proportion of magnetite in igneous rocks tends to decrease with increasing acidity so that acid igneous rocks, although variable in their magnetic behaviour, are usually less magnetic than basic rocks. Metamorphic rocks are also variable in their magnetic character. If the partial pressure of oxygen is relatively low, magnetite becomes resorbed and the iron and oxygen are incorporated into other mineral phases as the grade of metamorphism increases. Relatively high oxygen partial pressure can, however, result in the formation of magnetite as an accessory mineral in metamorphic reactions.

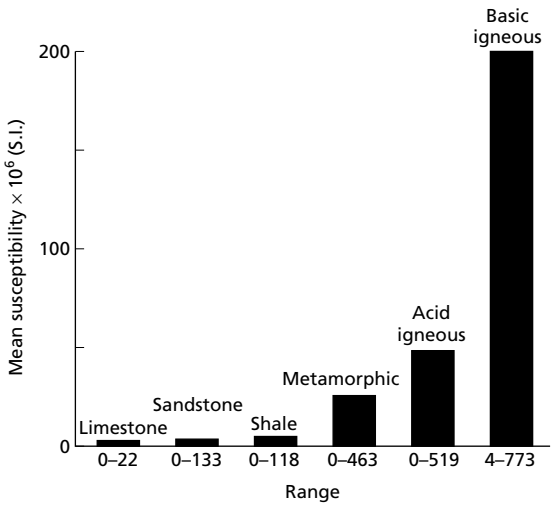

Fig. 7.5 Histogram showing mean values and ranges in susceptibility of common rock types. (After Dobrin & Savit 1988).

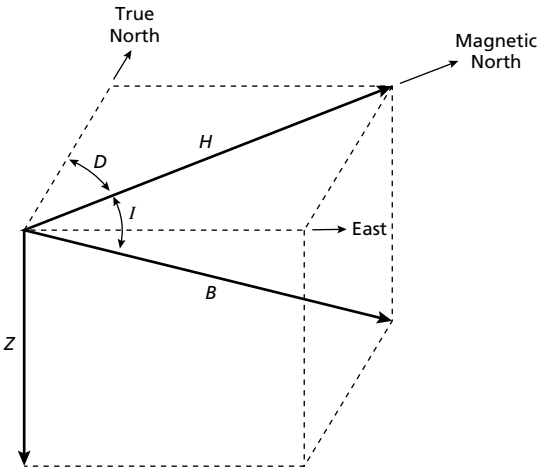

Fig. 7.6 The geomagnetic elements.

In general the magnetite content and, hence, the susceptibility of rocks is extremely variable and there can be considerable overlap between different lithologies. It is not usually possible to identify with certainty the causative lithology of any anomaly from magnetic information alone. However, sedimentary rocks are effectively non-magnetic unless they contain a significant amount of magnetite in the heavy mineral fraction. Where magnetic anomalies are observed over sediment-covered areas the anomalies are generally caused by an underlying igneous or metamorphic basement, or by intrusions into the sediments.

Common causes of magnetic anomalies include dykes, faulted, folded or truncated sills and lava flows, massive basic intrusions, metamorphic basement rocks and magnetite ore bodies. Magnetic anomalies range in amplitude from a few tens of nT over deep metamorphic basement to several hundred nT over basic intrusions and may reach an amplitude of several thousand nT over magnetite ores.

7.4 The geomagnetic field

Magnetic anomalies caused by rocks are localized effects superimposed on the normal magnetic field of the Earth (geomagnetic field). Consequently, knowledge of the behaviour of the geomagnetic field is necessary both in the reduction of magnetic data to a suitable datum and in the interpretation of the resulting anomalies. The geomagnetic field is geometrically more complex than the gravity field of the Earth and exhibits irregular variation in both orientation and magnitude with latitude, longitude and time.

At any point on the Earth's surface a freely suspended magnetic needle will assume a position in space in the direction of the ambient geomagnetic field. This will generally be at an angle to both the vertical and geographic north. In order to describe the magnetic field vector, use is made of descriptors known as the geomagnetic elements (Fig. 7.6). The *total field vector B* has a vertical component *Z* and a horizontal component *H* in the direction of magnetic north. The dip of *B* is the *inclination I* of the field and the horizontal angle between geographic and magnetic north is the *declination D*. *B* varies in strength from about 25 000 nT in equatorial regions to about 70 000 nT at the poles.

In the northern hemisphere the magnetic field generally dips downward towards the north and becomes vertical at the north magnetic pole (Fig. 7.7). In the southern hemisphere the dip is generally upwards towards the north. The line of zero inclination approximates the geographic equator, and is known as the magnetic equator.

About 90% of the Earth's field can be represented by the field of a theoretical magnetic dipole at the centre of the Earth inclined at about 11.5° to the axis of rotation. The magnetic moment of this fictitious *geocentric dipole* can be calculated from the observed field. If this dipole field is subtracted from the observed magnetic field, the

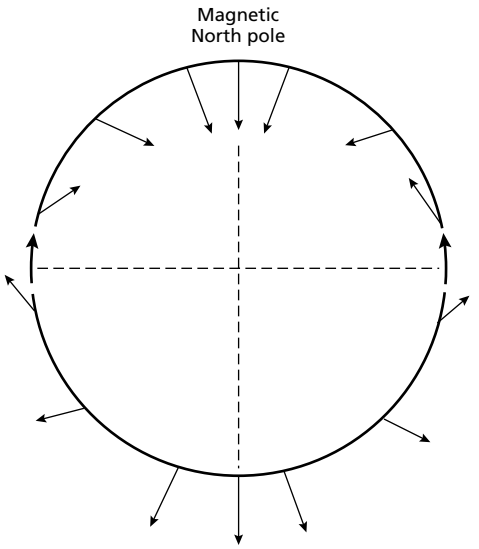

Fig. 7.7 The variation of the inclination of the total magnetic field with latitude based on a simple dipole approximation of the geomagnetic field. (After Sharma 1976.)

residual field can then be approximated by the effects of a second, smaller, dipole. The process can be continued by fitting dipoles of ever decreasing moment until the observed geomagnetic field is simulated to any required degree of accuracy. The effects of each fictitious dipole contribute to a function known as a harmonic and the technique of successive approximations of the observed field is known as spherical harmonic analysis – the equivalent of Fourier analysis in spherical polar coordinates. The method has been used to compute the formula of the International Geomagnetic Reference Field (IGRF) which defines the theoretical undisturbed magnetic field at any point on the Earth's surface. In magnetic surveying, the IGRF is used to remove from the magnetic data those magnetic variations attributable to this theoretical field. The formula is considerably more complex than the equivalent Gravity Formula used for latitude correction (see Section 6.8.2) as a large number of harmonics is employed (Barraclough & Malin 1971, Peddie 1983).

The geomagnetic field cannot in fact result from permanent magnetism in the Earth's deep interior. The required dipolar magnetic moments are far greater than is considered realistic and the prevailing high temperatures are far in excess of the Curie temperature of any known magnetic material. The cause of the geomagnetic field is attributed to a dynamo action produced by the circulation of charged particles in coupled convective cells within the outer, fluid, part of the Earth's core. The exchange of dominance between such cells is believed to produce the periodic changes in polarity of the geomagnetic field revealed by palaeomagnetic studies. The circulation patterns within the core are not fixed and change slowly with time. This is reflected in a slow, progressive, temporal change in all the geomagnetic elements known as *secular variation*. Such variation is predictable and a well-known example is the gradual rotation of the north magnetic pole around the geographic pole.

Magnetic effects of external origin cause the geomagnetic field to vary on a daily basis to produce *diurnal variations*. Under normal conditions (Q or quiet days) the diurnal variation is smooth and regular and has an amplitude of about 20–80 nT, being at a maximum in polar regions. Such variation results from the magnetic field induced by the flow of charged particles within the ionosphere towards the magnetic poles, as both the circulation patterns and diurnal variations vary in sympathy with the tidal effects of the Sun and Moon.

Some days (D or disturbed days) are distinguished by far less regular diurnal variations and involve large, short-term disturbances in the geomagnetic field, with amplitudes of up to 1000 nT, known as *magnetic storms*. Such days are usually associated with intense solar activity and result from the arrival in the ionosphere of charged solar particles. Magnetic surveying should be discontinued during such storms because of the impossibility of correcting the data collected for the rapid and high-amplitude changes in the magnetic field.

7.5 Magnetic anomalies

All magnetic anomalies caused by rocks are superimposed on the geomagnetic field in the same way that gravity anomalies are superimposed on the Earth's gravitational field. The magnetic case is more complex, however, as the geomagnetic field varies not only in amplitude, but also in direction, whereas the gravitational field is everywhere, by definition, vertical.

Describing the normal geomagnetic field by a vector diagram (Fig. 7.8(a)), the geomagnetic elements are related

$$B^2 = H^2 + Z^2 \tag{7.7}$$

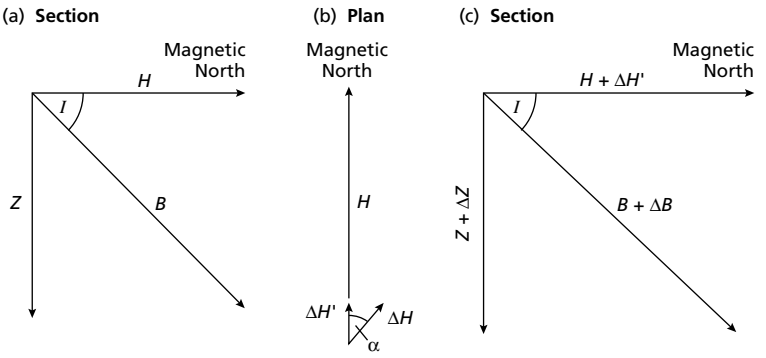

Fig. 7.8 Vector representation of the geomagnetic field with and without a superimposed magnetic anomaly.

A magnetic anomaly is now superimposed on the Earth's field causing a change ΔB in the strength of the total field vector B. Let the anomaly produce a vertical component ΔZ and a horizontal component ΔH at an angle α to H (Fig. 7.8(b)). Only that part of ΔH in the direction of H, namely $\Delta H'$, will contribute to the anomaly

$$\Delta H' = \Delta H \cos\alpha \tag{7.8}$$

Using a similar vector diagram to include the magnetic anomaly (Fig. 7.8(c))

$$(B + \Delta B)^2 = (H + \Delta H')^2 + (Z + \Delta Z)^2$$

If this equation is expanded, the equality of equation (7.7) substituted and the insignificant terms in Δ^2 ignored, the equation reduces to

$$\Delta B = \Delta Z \frac{Z}{B} + \Delta H' \frac{H}{B}$$

Substituting equation (7.8) and angular descriptions of geomagnetic element ratios gives

$$\Delta B = \Delta Z \sin I + \Delta H \cos I \cos\alpha \tag{7.9}$$

where I is the inclination of the geomagnetic field.

This approach can be used to calculate the magnetic anomaly caused by a small isolated magnetic pole of strength m, defined as the effect of this pole on a unit positive pole at the observation point. The pole is situated at depth z, a horizontal distance x and radial distance r from the observation point (Fig. 7.9). The force of repulsion ΔB_r on the unit positive pole in the direction r is given by substitution in equation (7.1), with $\mu_R = 1$,

$$\Delta B_r = \frac{Cm}{r^2}$$

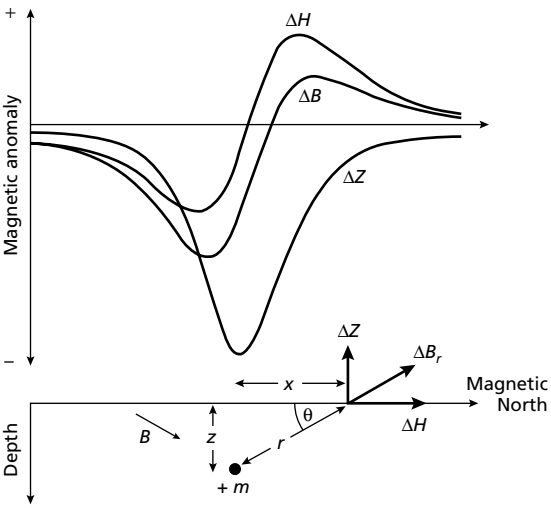

Fig. 7.9 The horizontal (ΔH), vertical (ΔZ) and total field (ΔB) anomalies due to an isolated positive pole.

where $C = \dfrac{\mu_0}{4\pi}$

If it is assumed that the profile lies in the direction of magnetic north so that the horizontal component of the anomaly lies in this direction, the horizontal (ΔH) and vertical (ΔZ) components of this force can be computed by resolving in the relevant directions

$$\Delta H = \frac{Cm}{r^2}\cos\theta = \frac{Cmx}{r^3} \tag{7.10}$$

$$\Delta Z = \frac{-Cm}{r^2}\sin\theta = \frac{-Cmz}{r^3} \tag{7.11}$$

The vertical field anomaly is negative as, by convention, the z-axis is positive downwards. Plots of the form of these anomalies are shown in Fig. 7.9. The horizontal

field anomaly is a positive/negative couplet and the vertical field anomaly is centred over the pole.

The total field anomaly ΔB is then obtained by substituting the expressions of equations (7.10) and (7.11) in equation (7.9), where $\alpha = 0$. If the profile were not in the direction of magnetic north, the angle α would represent the angle between magnetic north and the profile direction.

7.6 Magnetic surveying instruments

7.6.1 Introduction

Since the early 1900s a variety of surveying instruments have been designed that is capable of measuring the geomagnetic elements Z, H and B. Most modern survey instruments, however, are designed to measure B only. The precision normally required is ± 0.1 nT which is approximately one part in 5×10^6 of the background field, a considerably lower requirement of precision than is necessary for gravity measurements (see Chapter 6).

In early magnetic surveys the geomagnetic elements were measured using *magnetic variometers*. There were several types, including the torsion head magnetometer and the Schmidt vertical balance, but all consisted essentially of bar magnets suspended in the Earth's field. Such devices required accurate levelling and a stable platform for measurement so that readings were time consuming and limited to sites on land.

7.6.2 Fluxgate magnetometer

Since the 1940s, a new generation of instruments has been developed which provides virtually instantaneous readings and requires only coarse orientation so that magnetic measurements can be taken on land, at sea and in the air.

The first such device to be developed was the *fluxgate magnetometer*, which found early application during the second world war in the detection of submarines from the air. The instrument employs two identical ferromagnetic cores of such high permeability that the geomagnetic field can induce a magnetization that is a substantial proportion of their saturation value (see Section 7.2). Identical primary and secondary coils are wound in opposite directions around the cores (Fig. 7.10). An alternating current of 50–1000 Hz is passed through the primary coils (Fig. 7.10(a)), generating an alternating magnetic field. In the absence of any external magnetic field, the cores are driven to saturation near the peak of each half-cycle of the current (Fig. 7.10(b)). The alternating magnetic field in the cores induces an alternating voltage in the secondary coils which is at a maximum when the field is changing most rapidly (Fig. 7.10(c)). Since the coils are wound in opposite directions, the

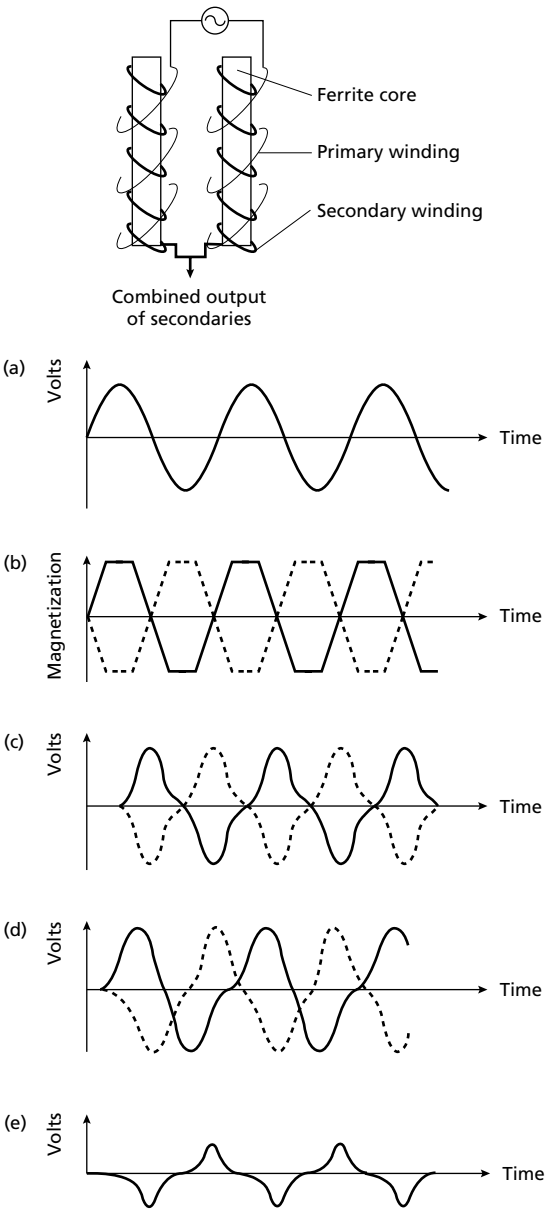

Fig. 7.10 Principle of the fluxgate magnetometer. Solid and broken lines in (b)–(d) refer to the responses of the two cores.

voltage in the coils is equal and of opposite sign so that their combined output is zero. In the presence of an external magnetic field, such as the Earth's field, which has a component parallel to the axis of the cores, saturation occurs earlier for the core whose primary field is reinforced by the external field and later for the core opposed by the external field. The induced voltages are now out of phase as the cores reach saturation at different times (Fig. 7.10(d)). Consequently, the combined output of the secondary coils is no longer zero but consists of a series of voltage pulses (Fig. 7.10(e)), the magnitude of which can be shown to be proportional to the amplitude of the external field component.

The instrument can be used to measure Z or H by aligning the cores in these directions, but the required accuracy of orientation is some eleven seconds of arc to achieve a reading accuracy of ± 1 nT. Such accuracy is difficult to obtain on the ground and impossible when the instrument is mobile. The total geomagnetic field can, however, be measured to ± 1 nT with far less precise orientation as the field changes much more slowly as a function of orientation about the total field direction. Airborne versions of the instrument employ orienting mechanisms of various types to maintain the axis of the instrument in the direction of the geomagnetic field. This is accomplished by making use of the feedback signal generated by additional sensors whenever the instrument moves out of orientation to drive servomotors which realign the cores into the desired direction.

The fluxgate magnetometer is a continuous reading instrument and is relatively insensitive to magnetic field gradients along the length of the cores. The instrument may be temperature sensitive, requiring correction.

7.6.3 Proton magnetometer

The most commonly used magnetometer for both survey work and observatory monitoring is currently the *nuclear precession* or *proton magnetometer*. The sensing device of the proton magnetometer is a container filled with a liquid rich in hydrogen atoms, such as kerosene or water, surrounded by a coil (Fig. 7.11(a)). The hydrogen nuclei (protons) act as small dipoles and normally align parallel to the ambient geomagnetic field B_e (Fig. 7.11(b)). A current is passed through the coil to generate a magnetic field B_p 50–100 times larger than the geomagnetic field, and in a different direction, causing the protons to realign in this new direction (Fig. 7.11(c)). The current to the coil is then switched off so that the

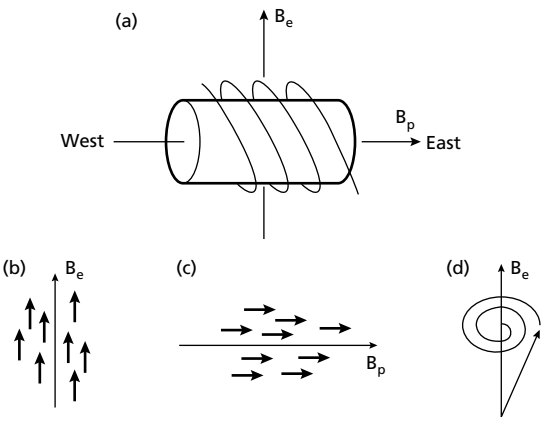

Fig. 7.11 Principle of the proton magnetometer.

polarizing field is rapidly removed. The protons return to their original alignment with B_e by spiralling, or precessing, in phase around this direction (Fig. 7.11(d)) with a period of about 0.5 ms, taking some 1–3 s to achieve their original orientation. The frequency f of this precession is given by

$$f = \frac{\gamma_p B_e}{2\pi}$$

where γ_p is the gyromagnetic ratio of the proton, an accurately known constant. Consequently, measurement of f, about 2 kHz, provides a very accurate measurement of the strength of the total geomagnetic field. f is determined by measurement of the alternating voltage of the same frequency induced to flow in the coil by the precessing protons.

Field instruments provide absolute readings of the total magnetic field accurate to ± 0.1 nT although much greater precision can be attained if necessary. The sensor does not have to be accurately oriented, although it should ideally lie at an appreciable angle to the total field vector. Consequently, readings may be taken by sensors towed behind ships or aircraft without the necessity of orienting mechanisms. Aeromagnetic surveying with proton magnetometers may suffer from the slight disadvantage that readings are not continuous due to the finite cycle period. Small anomalies may be missed since an aircraft travels a significant distance between the discrete measurements, which may be spaced at intervals of a few seconds. This problem has been largely obviated by modern instruments with recycling periods of the order

of a second. The proton magnetometer is sensitive to acute magnetic gradients which may cause protons in different parts of the sensor to precess at different rates with a consequent adverse effect on precession signal strength.

Many modern proton magnetometers make use of the *Overhauser Effect*. To the sensor fluid is added a liquid containing some free electrons in 'unpaired' orbits. The protons are then polarized indirectly using radio-frequency energy near 60 MHz. The power consumption of such instruments is only some 25% of classical proton magnetometers, so that the instruments are lighter and more compact. The signal generated by the fluid is about 100 times stronger, so there is much lower noise; gradient tolerance is some three times better; sampling rates are faster.

7.6.4 Optically pumped magnetometer

Optically pumped or *alkali vapour magnetometers* have a significantly higher precision than other types. They comprise a glass cell containing an evaporated alkali metal such as caesium, rubidium or potassium which is energized by light of a particular wavelength. In these alkali atoms there exist valence electrons partitioned into two energy levels 1 and 2. The wavelength of the energizing light is selected to excite electrons from level 2 to the higher level 3, a process termed polarization. Electrons at level 3 are unstable and spontaneously decay back to levels 1 and 2. As this process is repeated, level 1 becomes fully populated at the expense of level 2 becoming underpopulated. This process is known as optical pumping and leads to the stage in which the cell stops absorbing light and turns from opaque to transparent. The energy difference between levels 1 and 2 is proportional to the strength of the ambient magnetic field. Depolarization then takes place by the application of radio-frequency power. The wavelength corresponding to the energy difference between levels 1 and 2 depolarizes the cell and is a measure of the magnetic field strength. A photodetector is used to balance the cell between transparent and opaque states. The depolarization is extremely rapid so that readings are effectively instantaneous. The sensitivity of optically pumped magnetometers can be as high as ±0.01 nT. This precision is not required for surveys involving total field measurements, where the level of background 'noise' is of the order of 1 nT. The usual application is in the magnetic gradiometers described below, which rely on measuring the small difference in signal from sensors only a small distance apart.

7.6.5 Magnetic gradiometers

The sensing elements of fluxgate, proton and optically pumped magnetometers can be used in pairs to measure either horizontal or vertical magnetic field gradients. *Magnetic gradiometers* are differential magnetometers in which the spacing between the sensors is fixed and small with respect to the distance of the causative body whose magnetic field gradient is to be measured. Magnetic gradients can be measured, albeit less conveniently, with a magnetometer by taking two successive measurements at close vertical or horizontal spacings. Magnetic gradiometers are employed in surveys of shallow magnetic features as the gradient anomalies tend to resolve complex anomalies into their individual components, which can be used in the determination of the location, shape and depth of the causative bodies. The method has the further advantages that regional and temporal variations in the geomagnetic field are automatically removed. Marine and airborne versions of magnetometers and gradiometers are discussed by Wold and Cooper (1989) and Hood and Teskey (1989), respectively.

7.7 Ground magnetic surveys

Ground magnetic surveys are usually performed over relatively small areas on a previously defined target. Consequently, station spacing is commonly of the order of 10–100 m, although smaller spacings may be employed where magnetic gradients are high. Readings should not be taken in the vicinity of metallic objects such as railway lines, cars, roads, fencing, houses, etc, which might perturb the local magnetic field. For similar reasons, operators of magnetometers should not carry metallic objects.

Base station readings are not necessary for monitoring instrumental drift as fluxgate and proton magnetometers do not drift, but are important in monitoring diurnal variations (see Section 7.9).

Since modern magnetic instruments require no precise levelling, a magnetic survey on land invariably proceeds much more rapidly than a gravity survey.

7.8 Aeromagnetic and marine surveys

The vast majority of magnetic surveys are carried out in the air, with the sensor towed in a housing known as

a 'bird' to remove the instrument from the magnetic effects of the aircraft or fixed in a 'stinger' in the tail of the aircraft, in which case inboard coil installations compensate for the aircraft's magnetic field.

Aeromagnetic surveying is rapid and cost-effective, typically costing some 40% less per line kilometre than a ground survey. Vast areas can be surveyed rapidly without the cost of sending a field party into the survey area and data can be obtained from areas inaccessible to ground survey.

The most difficult problem in airborne surveys used to be position fixing. Nowadays, however, the availability of GPS obviates the positioning problem.

Marine magnetic surveying techniques are similar to those of airborne surveying. The sensor is towed in a 'fish' at least two ships' lengths behind the vessel to remove its magnetic effects. Marine surveying is obviously slower than aeromagnetic surveying, but is frequently carried out in conjunction with several other geophysical methods, such as gravity surveying and continuous seismic profiling, which cannot be employed in the air.

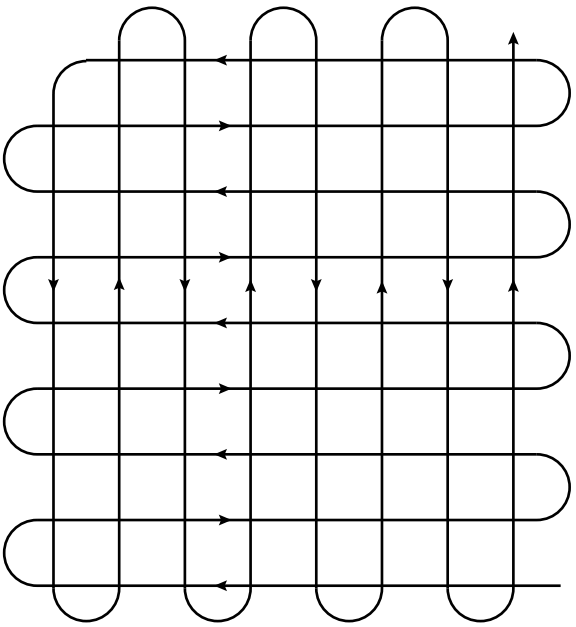

Fig. 7.12 A typical flight plan for an aeromagnetic survey.

7.9 Reduction of magnetic observations

The reduction of magnetic data is necessary to remove all causes of magnetic variation from the observations other than those arising from the magnetic effects of the subsurface.

7.9.1 Diurnal variation correction

The effects of diurnal variation may be removed in several ways. On land a method similar to gravimeter drift monitoring may be employed in which the magnetometer is read at a fixed base station periodically throughout the day. The differences observed in base readings are then distributed among the readings at stations occupied during the day according to the time of observation. It should be remembered that base readings taken during a gravity survey are made to correct for both the drift of the gravimeter and tidal effects; magnetometers do not drift and base readings are taken solely to correct for temporal variation in the measured field. Such a procedure is inefficient as the instrument has to be returned periodically to a base location and is not practical in marine or airborne surveys. These problems may be overcome by use of a base magnetometer, a continuous-reading instrument which records magnetic variations at a fixed location within or close to the survey area. This method is preferable on land as the survey proceeds faster and the diurnal variations are fully charted. Where the survey is of regional extent the records of a magnetic observatory may be used. Such observatories continuously record changes in all the geomagnetic elements. However, diurnal variations differ quite markedly from place to place and so the observatory used should not be more than about 100 km from the survey area.

Diurnal variation during an aeromagnetic survey may alternatively be assessed by arranging numerous crossover points in the survey plan (Fig. 7.12). Analysis of the differences in readings at each crossover, representing the field change over a series of different time periods, allows the whole survey to be corrected for diurnal variation by a process of network adjustment, without the necessity of a base instrument.

Diurnal variations, however recorded, must be examined carefully. If large, high-frequency variations are apparent, resulting from a magnetic storm, the survey results should be discarded.

7.9.2 Geomagnetic correction

The magnetic equivalent of the latitude correction in gravity surveying is the *geomagnetic correction* which removes the effect of a geomagnetic reference field from the survey data. The most rigorous method of geomagnetic correction is the use of the IGRF (Section 7.4), which expresses the undisturbed geomagnetic field in terms of a large number of harmonics and includes temporal terms to correct for secular variation. The complexity of the IGRF requires the calculation of corrections by computer. It must be realized, however, that the IGRF is imperfect as the harmonics employed are based on observations at relatively few, scattered, magnetic observatories. The IGRF is also predictive in that it extrapolates forwards the spherical harmonics derived from observatory data. Consequently, the IGRF in areas remote from observatories can be substantially in error.

Over the area of a magnetic survey the geomagnetic reference field may be approximated by a uniform gradient defined in terms of latitudinal and longitudinal gradient components. For example, the geomagnetic field over the British Isles is approximated by the following gradient components: $2.13\,\mathrm{nT\,km^{-1}}$ N; $0.26\,\mathrm{nT\,km^{-1}}$ W; these vary with time. For any survey area the relevant gradient values may be assessed from magnetic maps covering a much larger region.

The appropriate regional gradients may also be obtained by employing a single dipole approximation of the Earth's field and using the well-known equations for the magnetic field of a dipole to derive local field gradients:

$$Z = \frac{\mu_0}{4\pi}\frac{2M}{R^3}\cos\theta, \qquad H = \frac{\mu_0}{4\pi}\frac{M}{R^3}\sin\theta \tag{7.12}$$

$$\frac{\partial Z}{\partial \theta} = -2H, \qquad \frac{\partial H}{\partial \theta} = \frac{Z}{2} \tag{7.13}$$

where Z and H are the vertical and horizontal field components, θ the colatitude in radians, R the radius of the Earth, M the magnetic moment of the Earth and $\partial Z/\partial\theta$ and $\partial H/\partial\theta$ the rate of change of Z and H with colatitude, respectively.

An alternative method of removing the regional gradient over a relatively small survey area is by use of trend analysis. A trend line (for profile data) or trend surface (for areal data) is fitted to the observations using the least squares criterion, and subsequently subtracted from the observed data to leave the local anomalies as positive and negative residuals (Fig. 7.13).

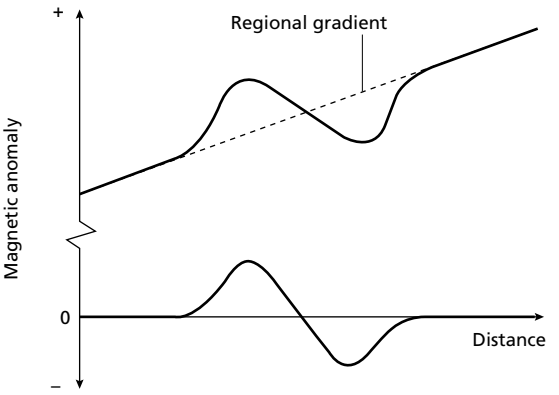

Fig. 7.13 The removal of a regional gradient from a magnetic field by trend analysis. The regional field is approximated by a linear trend.

7.9.3 Elevation and terrain corrections

The vertical gradient of the geomagnetic field is only some $0.03\,\mathrm{nT\,m^{-1}}$ at the poles and $-0.015\,\mathrm{nT\,m^{-1}}$ at the equator, so an *elevation correction* is not usually applied. The influence of topography can be significant in ground magnetic surveys but is not completely predictable as it depends upon the magnetic properties of the topographic features. Therefore, in magnetic surveying *terrain corrections* are rarely applied.

Having applied diurnal and geomagnetic corrections, all remaining magnetic field variations should be caused solely by spatial variations in the magnetic properties of the subsurface and are referred to as magnetic anomalies.

7.10 Interpretation of magnetic anomalies

7.10.1 Introduction

The interpretation of magnetic anomalies is similar in its procedures and limitations to gravity interpretation as both techniques utilize natural potential fields based on inverse square laws of attraction. There are several differences, however, which increase the complexity of magnetic interpretation.

Whereas the gravity anomaly of a causative body is entirely positive or negative, depending on whether the body is more or less dense than its surroundings, the magnetic anomaly of a finite body invariably contains positive and negative elements arising from the dipolar nature of magnetism (Fig. 7.14). Moreover, whereas

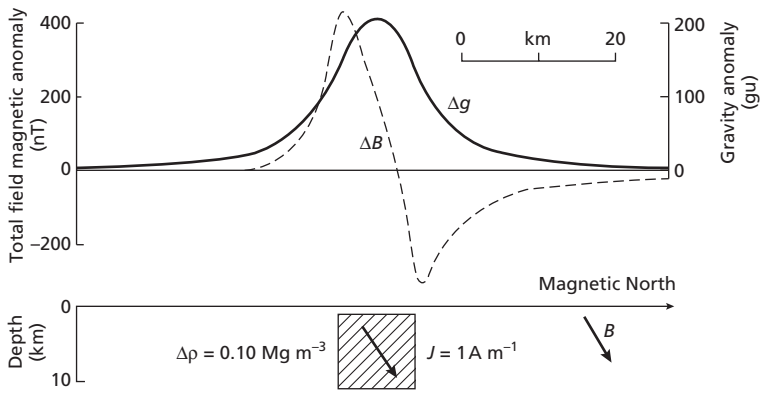

Fig. 7.14 Gravity (Δg) and magnetic (ΔB) anomalies over the same two-dimensional body.

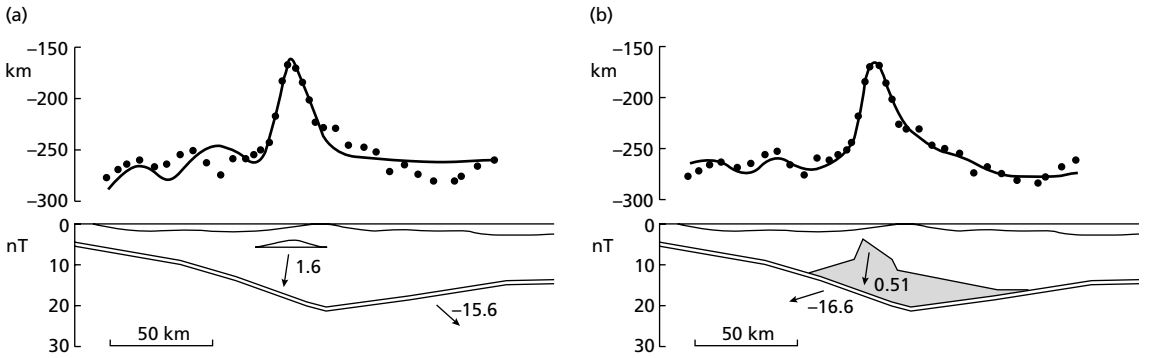

Fig. 7.15 An example of ambiguity in magnetic interpretation. The arrows correspond to the directions of magnetization vectors, whose magnitude is given in A m^{-1}. (After Westbrook 1975.)

density is a scalar, intensity of magnetization is a vector, and the direction of magnetization in a body closely controls the shape of its magnetic anomaly. Thus bodies of identical shape can give rise to very different magnetic anomalies. For the above reasons magnetic anomalies are often much less closely related to the shape of the causative body than are gravity anomalies.

The intensity of magnetization of a rock is largely dependent upon the amount, size, shape and distribution of its contained ferrimagnetic minerals and these represent only a small proportion of its constituents. By contrast, density is a bulk property. Intensity of magnetization can vary by a factor of 10^6 between different rock types, and is thus considerably more variable than density, where the range is commonly 1.50–3.50 Mg m^{-3}.

Magnetic anomalies are independent of the distance units employed. For example, the same magnitude anomaly is produced by, say, a 3 m cube (on a metre scale) as a 3 km cube (on a kilometre scale) with the same magnetic properties. The same is not true of gravity anomalies.

The problem of ambiguity in magnetic interpretation is the same as for gravity, that is, the same inverse problem is encountered. Thus, just as with gravity, all external controls on the nature and form of the causative body must be employed to reduce the ambiguity. An example of this problem is illustrated in Fig. 7.15, which shows two possible interpretations of a magnetic profile across the Barbados Ridge in the eastern Caribbean. In both cases the regional variations are attributed to the variation in depth of a 1 km thick oceanic crustal layer 2. The high-amplitude central anomaly, however, can be explained by either the presence of a detached sliver of oceanic crust (Fig. 7.15(a)) or a rise of metamorphosed sediments at depth (Fig. 7.15(b)).

Much qualitative information may be derived from a magnetic contour map. This applies especially to aeromagnetic maps which often provide major clues as to the

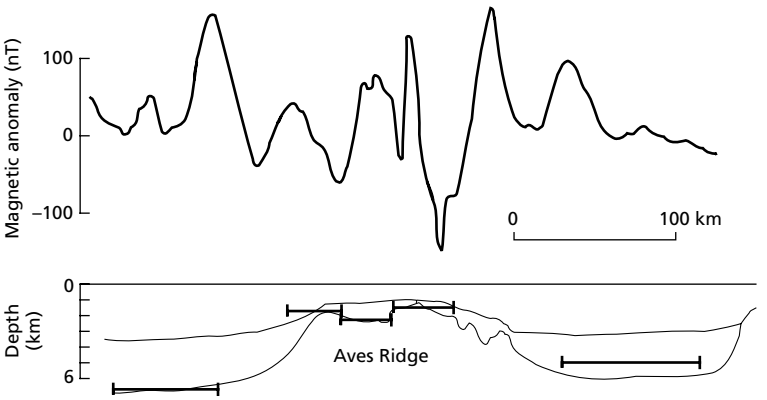

Fig. 7.16 Magnetic anomalies over the Aves Ridge, eastern Caribbean. Lower diagram illustrates bathymetry and basement/sediment interface. Horizontal bars indicate depth estimates of the magnetic basement derived by spectral analysis of the magnetic data.

geology and structure of a broad region from an assessment of the shapes and trends of anomalies. Sediment-covered areas with relatively deep basement are typically represented by smooth magnetic contours reflecting basement structures and magnetization contrasts. Igneous and metamorphic terrains generate far more complex magnetic anomalies, and the effects of deep geological features may be obscured by short-wavelength anomalies of near-surface origin. In most types of terrain an aeromagnetic map can be a useful aid to reconnaissance geological mapping. Such qualitative interpretations may be greatly facilitated by the use of digital image processing techniques (see Section 6.8.6).

In carrying out quantitative interpretation of magnetic anomalies, both direct and indirect methods may be employed, but the former are much more limited than for gravity interpretation and no equivalent general equations exist for total field anomalies.

7.10.2 Direct interpretation

Limiting depth is the most important parameter derived by direct interpretation, and this may be deduced from magnetic anomalies by making use of their property of decaying rapidly with distance from source. Magnetic anomalies caused by shallow structures are more dominated by short-wavelength components than those resulting from deeper sources. This effect may be quantified by computing the power spectrum of the anomaly as it can be shown, for certain types of source body, that the log-power spectrum has a linear gradient whose magnitude is dependent upon the depth of the source (Spector & Grant 1970). Such techniques of spectral analysis provide rapid depth estimates from regularly-spaced digital field data; no geomagnetic or diurnal corrections are necessary as these remove only low-wavenumber components and do not affect the depth estimates which are controlled by the high-wavenumber components of the observed field. Figure 7.16 shows a magnetic profile across the Aves Ridge in the eastern Caribbean. In this region the configuration of the sediment/basement interface is reasonably well known from both seismic reflection and refraction surveys. The magnetic anomalies clearly show their shortest wavelength over areas of relatively shallow basement, and this observation is quantified by the power spectral depth estimates (horizontal bars) which show excellent correlation with the known basement relief.

A more complex, but more rigorous method of determining the depth to magnetic sources derives from a technique known as *Euler deconvolution* (Reid *et al.* 1990). Euler's homogeneity relation can be written:

$$(x - x_0)\frac{\partial T}{\partial x} + (y - y_0)\frac{\partial T}{\partial y} + (z - z_0)\frac{\partial T}{\partial z} = N(B - T) \tag{7.14}$$

where (x_0, y_0, z_0) is the location of a magnetic source, whose total field magnetic anomaly at the point (x, y, z) is T and B is the regional field. N is a measure of the rate of change of a field with distance and assumes different values for different types of magnetic source. Equation (7.14) is solved by calculating or measuring the anomaly gradients for various areas of the anomaly and selecting a value for N. This method produces more rigorous depth estimates than other methods, but is considerably more difficult to implement. An example of an Euler deconvolution is shown in Fig. 7.17. The aeromagnetic field shown in Fig. 7.17(a) has the solutions shown in Fig. 17(b–d) for structural indices (N) of 0.0, 0.5 and 0.6

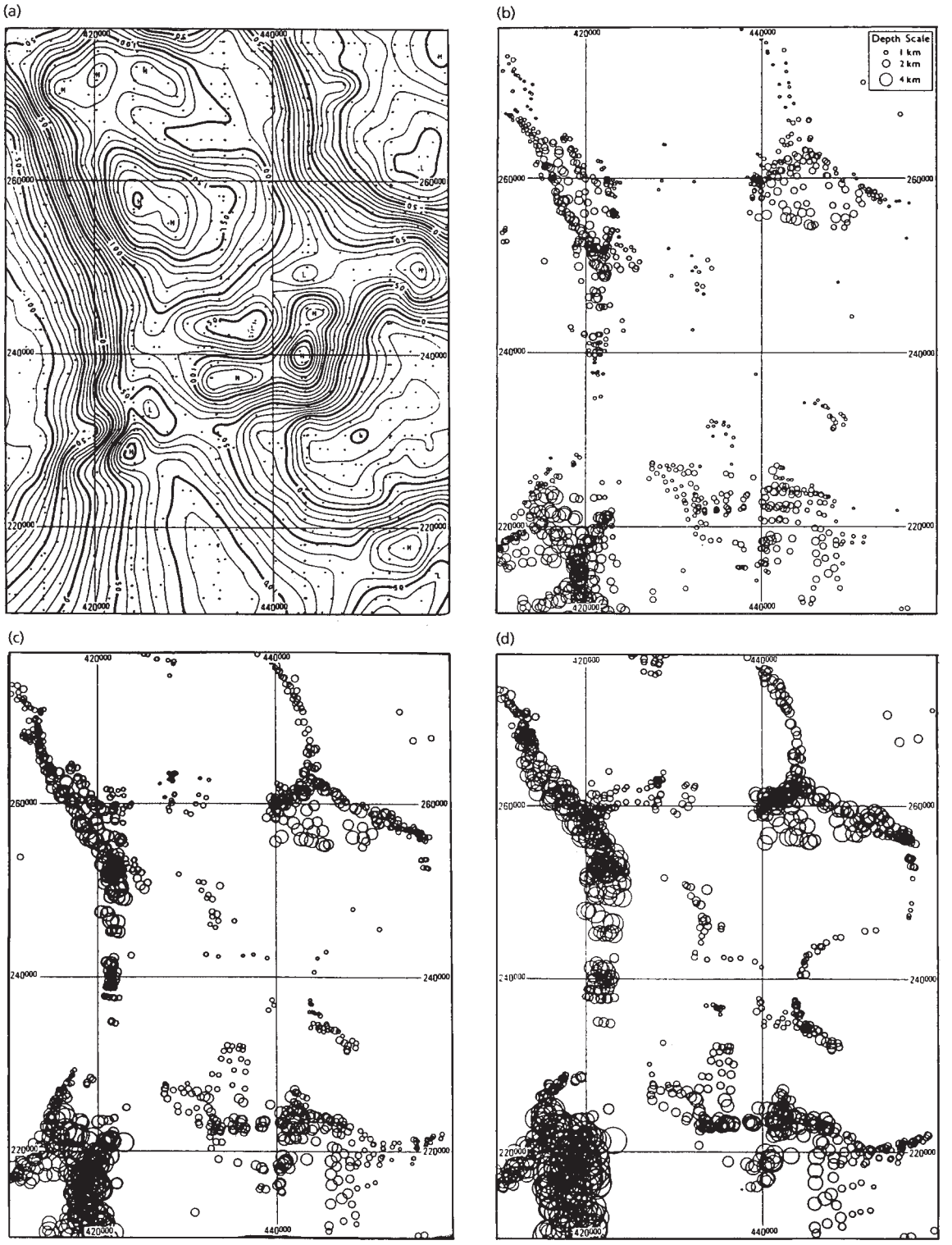

Fig. 7.17 (a) Observed aeromagnetic anomaly of a region in the English Midlands. Contour interval 10 nT. (b–d) Euler deconvolutions for structural indices 0.0 (b), 0.5 (c) and 1.0 (d). Source depth is indicated by the size of the circles. (e) Geological interpretation (*overleaf*). Grid squares are 10 km × 10 km in size. (After Reid *et al.* 1990.)

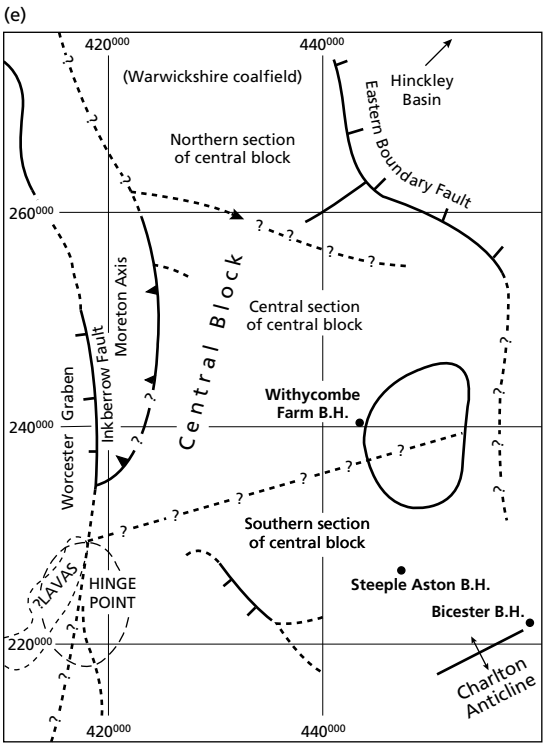

Fig. 7.17 *Continued*

respectively. The boundaries implied by the solutions have been used to construct the interpretation shown in Fig. 7.17(e).

7.10.3 Indirect interpretation

Indirect interpretation of magnetic anomalies is similar to gravity interpretation in that an attempt is made to match the observed anomaly with that calculated for a model by iterative adjustments to the model. Simple magnetic anomalies may be simulated by a single dipole. Such an approximation to the magnetization of a real geological body is often valid for highly magnetic ore bodies whose direction of magnetization tends to align with their long dimension (Fig. 7.18). In such cases the anomaly is calculated by summing the effects of both poles at the observation points, employing equations (7.10), (7.11) and (7.9). More complicated magnetic bodies, however, require a different approach.

The magnetic anomaly of most regularly-shaped bodies can be calculated by building up the bodies from a series of dipoles parallel to the magnetization direction

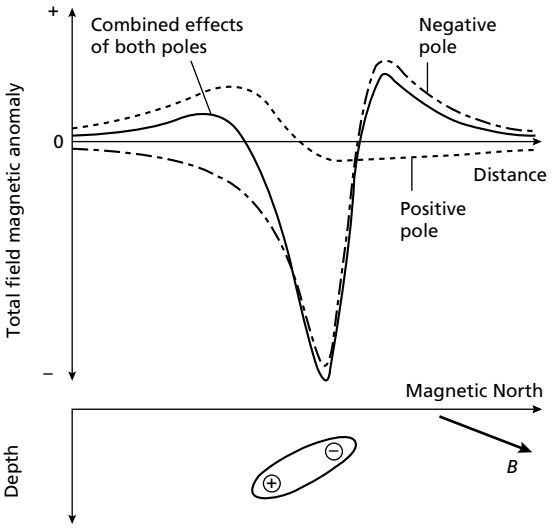

Fig. 7.18 The total field magnetic anomaly of an elongate body approximated by a dipole.

(Fig. 7.19). The poles of the magnets are negative on the surface of the body where the magnetization vector enters the body and positive where it leaves the body. Thus any uniformly-magnetized body can be represented by a set of magnetic poles distributed over its surface. Consider one of these elementary magnets of length l and cross-sectional area δA in a body with intensity of magnetization J and magnetic moment M. From equation (7.5)

$$M = J\delta A l \tag{7.15}$$

If the pole strength of the magnet is m, from equation (7.4) $m = M/l$, and substituting in equation (7.15)

$$m = J\delta A \tag{7.16}$$

If $\delta A'$ is the area of the end of the magnet and θ the angle between the magnetization vector and a direction normal to the end face

$$\delta A = \delta A' \cos\theta$$

Substituting in equation (7.16)

$$m = J\delta A' \cos\theta$$

thus

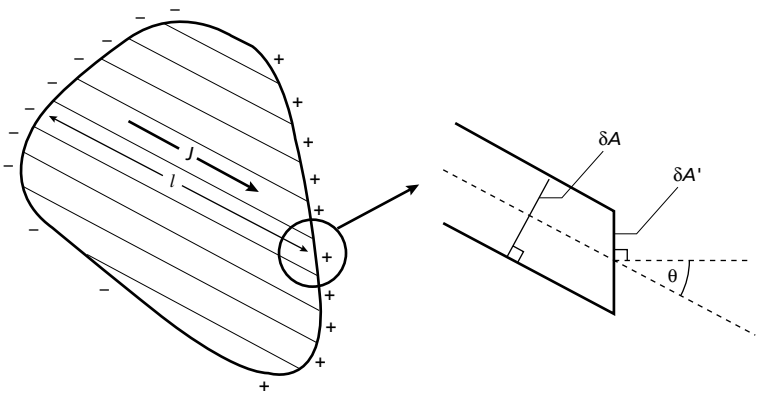

Fig. 7.19 The representation of the magnetic effects of an irregularly-shaped body in terms of a number of elements parallel to the magnetization direction. Inset shows in detail the end of one such element.

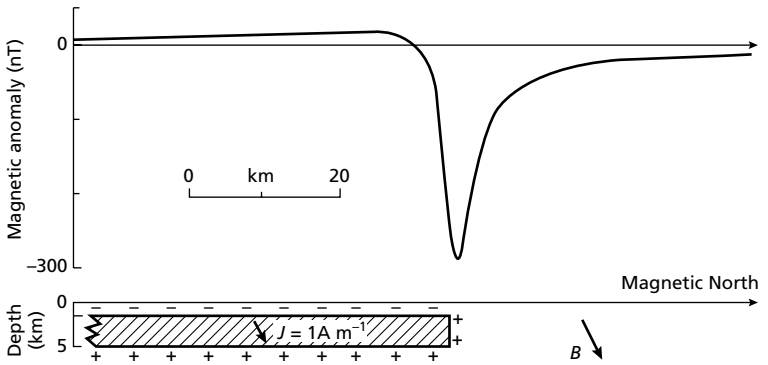

Fig. 7.20 The total field magnetic anomaly of a faulted sill.

$$\text{pole strength per unit area} = J\cos\theta \tag{7.17}$$

A consequence of the distribution of an equal number of positive and negative poles over the surface of a magnetic body is that an infinite horizontal layer produces no magnetic anomaly since the effects of the poles on the upper and lower surfaces are self-cancelling. Consequently, magnetic anomalies are not produced by continuous sills or lava flows. Where, however, the horizontal structure is truncated, the vertical edge will produce a magnetic anomaly (Fig. 7.20).

The magnetic anomaly of a body of regular shape is calculated by determining the pole distribution over the surface of the body using equation (7.17). Each small element of the surface is then considered and its vertical and horizontal component anomalies are calculated at each observation point using equations (7.10) and (7.11). The effects of all such elements are summed (integrated) to produce the vertical and horizontal anomalies for the whole body and the total field anomaly is calculated using equation (7.9). The integration can be performed analytically for bodies of regular shape, while irregularly-shaped bodies may be split into regular shapes and the integration performed numerically.

In two-dimensional modelling, an approach similar to gravity interpretation can be adopted (see Section 6.10.4) in which the cross-sectional form of the body is approximated by a polygonal outline. The anomaly of the polygon is then computed by adding or subtracting the anomalies of semi-infinite slabs with sloping edges corresponding to the sides of the polygon (Fig. 7.21). In the magnetic case, the horizontal ΔH, vertical ΔZ and total field ΔB anomalies (nT) of the slab shown in Fig. 7.21 are given by (Talwani *et al.* 1965)

$$\Delta Z = 200\sin\theta[J_x\{\sin\theta\log_e(r_2/r_1)+\phi\cos\theta\} + J_z\{\cos\theta\log_e(r_2/r_1)-\phi\sin\theta\}] \tag{7.18a}$$

$$\Delta H = 200\sin\theta[J_x\{\phi\sin\theta-\cos\theta\log_e(r_2/r_1)\} + J_z\{\phi\cos\theta+\sin\theta\log_e(r_2/r_1)\}]\sin\alpha \tag{7.18b}$$

$$\Delta B = \Delta Z\sin I + \Delta H\cos I \tag{7.18c}$$

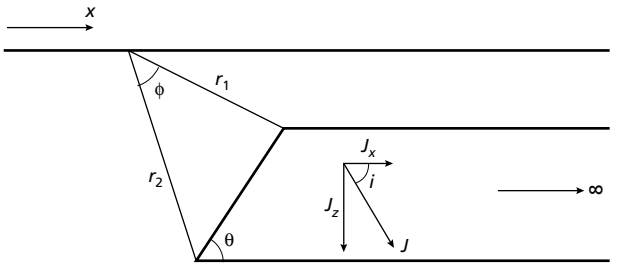

Fig. 7.21 Parameters used in defining the magnetic anomaly of a semi-infinite slab with a sloping edge.

where angles are expressed in radians, J_x ($= J\cos i$) and J_z ($= J\sin i$) are the horizontal and vertical components of the magnetization J, α is the horizontal angle between the direction of the profile and magnetic north, and I is the inclination of the geomagnetic field. Examples of this technique have been presented in Fig. 7.15. An important difference from gravity interpretation is the increased stringency with which the two-dimensional approximation should be applied. It can be shown that two-dimensional magnetic interpretation is much more sensitive to errors associated with variation along strike than is the case with gravity interpretation; the length–width ratio of a magnetic anomaly should be at least 10 : 1 for a two-dimensional approximation to be valid, in contrast to gravity interpretation where a 2 : 1 length–width ratio is sufficient to validate two-dimensional interpretation.

Three-dimensional modelling of magnetic anomalies is complex. Probably the most convenient methods are to approximate the causative body by a cluster of right rectangular prisms or by a series of horizontal slices of polygonal outline.

Because of the dipolar nature of magnetic anomalies, trial and error methods of indirect interpretation are difficult to perform manually since anomaly shape is not closely related to the geometry of the causative body. Consequently, the automatic methods of interpretation described in Section 6.10.3 are widely employed.

The continuation and filtering operations used in gravity interpretation and described in Section 6.11 are equally applicable to magnetic fields. A further processing operation that may be applied to magnetic anomalies is known as *reduction to the pole*, and involves the conversion of the anomalies into their equivalent form at the north magnetic pole (Baranov & Naudy 1964). This process usually simplifies the magnetic anomalies as the ambient field is then vertical and bodies with magnetizations which are solely induced produce anomalies that are axisymmetric. The existence of remanent magnetization, however, commonly prevents reduction to the pole from producing the desired simplification in the resultant pattern of magnetic anomalies.

7.11 Potential field transformations

The formulae for the gravitational potential caused by a point mass and the magnetic potential due to an isolated pole were presented in equations (6.3) and (7.3). A consequence of the similar laws of attraction governing gravitating and magnetic bodies is that these two equations have the variable of inverse distance ($1/r$) in common. Elimination of this term between the two formulae provides a relationship between the gravitational and magnetic potentials known as *Poisson's equation*. In reality the relationship is more complex than implied by equations (6.3) and (7.3) as isolated magnetic poles do not exist. However, the validity of the relationship between the two potential fields remains. Since gravity or magnetic fields can be determined by differentiation of the relevant potential in the required direction, Poisson's equation provides a method of transforming magnetic fields into gravitational fields and *vice versa* for bodies in which the ratio of intensity of magnetization to density remains constant. Such transformed fields are known as *pseudogravitational* and *pseudomagnetic* fields (Garland 1951).

One application of this technique is the transformation of magnetic anomalies into pseudogravity anomalies for the purposes of indirect interpretation, as the latter are significantly easier to interpret than their magnetic counterpart. The method is even more powerful when the pseudofield is compared with a corresponding measured field. For example, the comparison of gravity anomalies with the pseudogravity anomalies derived from magnetic anomalies over the same area can show whether the same geological bodies are the cause of the two types of anomaly. Performing the transformation for

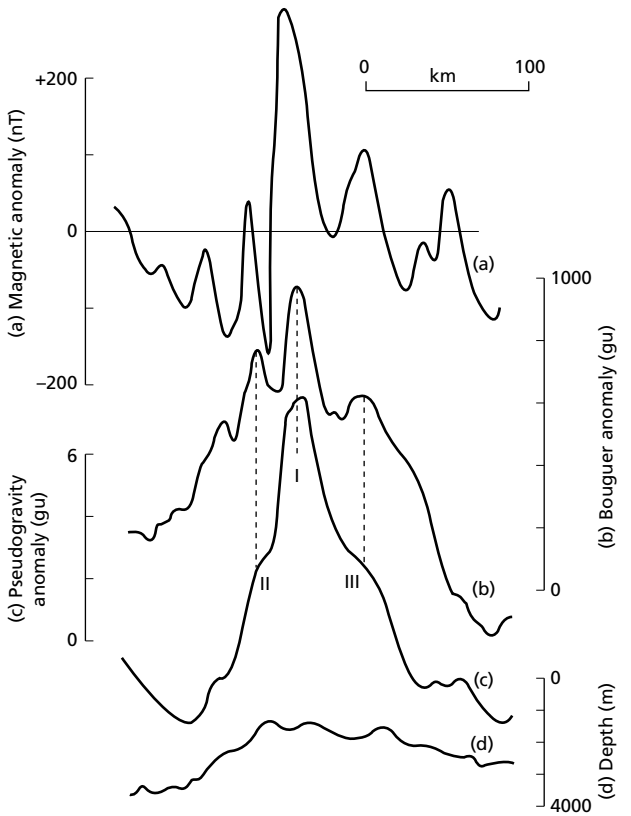

Fig. 7.22 (a) Observed magnetic anomalies over the Aves Ridge, eastern Caribbean. (b) Bouguer gravity anomalies with long-wavelength regional field removed. (c) Pseudogravity anomalies computed for induced magnetization and a density : magnetization ratio of unity. (d) Bathymetry.

different orientations of the magnetization vector provides an estimate of the true vector orientation since this will produce a pseudogravity field which most closely approximates the observed gravity field. The relative amplitudes of these two fields then provide a measure of the ratio of intensity of magnetization to density (Ates & Kearey 1995). These potential field transformations provide an elegant means of comparing gravity and magnetic anomalies over the same area and sometimes allow greater information to be derived about their causative bodies than would be possible if the techniques were treated in isolation. A computer program which performs pseudofield transformations is given in Gilbert and Galdeano (1985).

Figures 7.22(a) and (b) show magnetic and residual gravity anomaly profiles across the Aves Ridge, a submarine prominence in the eastern Caribbean which runs parallel to the island arc of the Lesser Antilles. The pseudogravity profile calculated from the magnetic profile assuming induced magnetization is presented in Fig. 7.22(c). It is readily apparent that the main pseudogravity peak correlates with peak I on the gravity profile and that peaks II and III correlate with much weaker features on the pseudofield profile. The data thus suggest that the density features responsible for the gravity maxima are also magnetic, with the causative body of the central peak having a significantly greater susceptibility than the flanking bodies.

Figure 7.23 shows how a variety of processing methods can be used on a synthetic magnetic anomaly map and Fig. 7.24 shows their application to real data.

7.12 Applications of magnetic surveying

Magnetic surveying is a rapid and cost-effective technique and represents one of the most widely-used geophysical methods in terms of line length surveyed (Paterson & Reeves 1985).

Magnetic surveys are used extensively in the search for metalliferous mineral deposits, a task accomplished rapidly and economically by airborne methods.

Magnetic surveys are capable of locating massive sulphide deposits (Fig. 7.25), especially when used in conjunction with electromagnetic methods (see Section 9.12). However, the principal target of magnetic surveying is iron ore. The ratio of magnetite to haematite must be high for the ore to produce significant anomalies, as haematite is commonly non-magnetic (see Section 7.2). Figure 7.26 shows total field magnetic anomalies from an airborne survey of the Northern Middleback Range, South Australia, in which it is seen that the haematitic ore bodies are not associated with the major anomalies. Figure 7.27 shows the results from an aeromagnetic survey of part of the Eyre Peninsula of South Australia which reveal the presence of a large anomaly elongated east–west. Subsequent ground traverses were performed over this anomaly using both magnetic and gravity methods (Fig. 7.28) and it was found that the magnetic and gravity profiles exhibit coincident highs. Subsequent drilling on these highs revealed the presence of a magnetite-bearing ore body at shallow depth with an iron content of about 30%.

Gunn (1998) has reported on the location of prospective areas for hydrocarbon deposits in Australia by aeromagnetic surveying, although it is probable that this application is only possible in quite specific environments.

In geotechnical and archaeological investigations, magnetic surveys may be used to delineate zones of faulting in bedrock and to locate buried metallic, man-made features such as pipelines, old mine workings and buildings. Figure 7.29 shows a total magnetic field contour map of the site of a proposed apartment block in Bristol, England. The area had been exploited for coal in the past and stability problems would arise from the presence of old shafts and buried workings (Clark 1986). Lined shafts of up to 2 m diameter were subsequently found beneath anomalies A and D, while other isolated anomalies such as B and C were known, or suspected, to be associated with buried metallic objects.

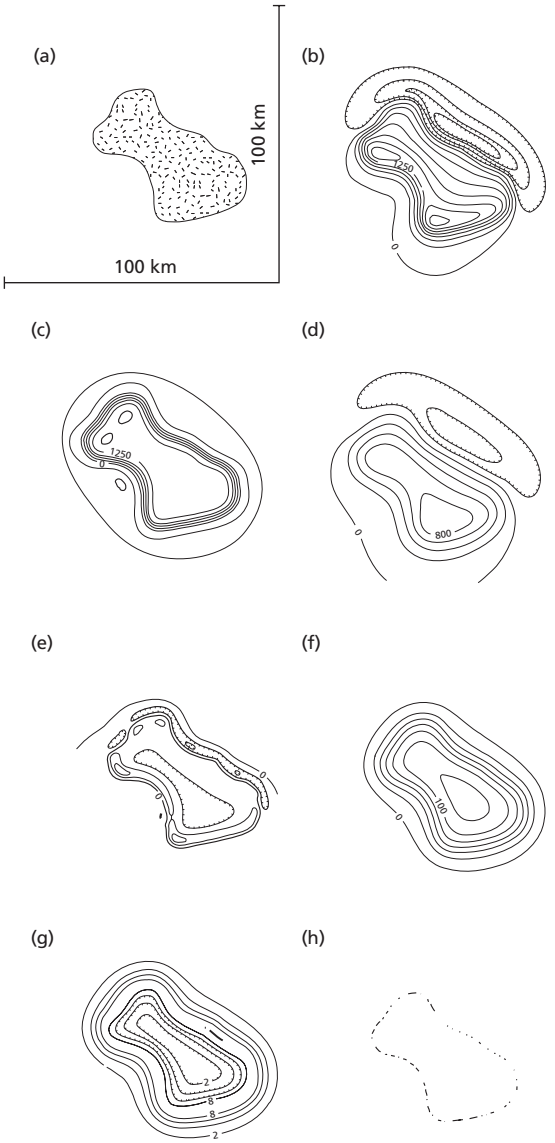

Fig. 7.23 The processing of aeromagnetic data. North direction is from bottom to top. (a) Source body with vertical sides, 2 km thick and a magnetization of 10 A m^{-1}, inclination 60° and declination 20°. (b) Total field magnetic anomaly of the body with induced magnetization measured on a horizontal surface 4 km above the body. Contour interval 250 nT. (c) Reduction to the pole of anomaly shown in (b). Contour interval 250 nT. (d) Anomaly shown in (b) upward continued 5 km above the measurement surface. Contour interval 200 nT. (e) Second vertical derivative of the anomaly shown in (b). Contour interval 50 nT km^{-2}. (f) Pseudogravity transform of anomaly shown in (b) assuming an intensity of magnetization of 1 A m^{-1} and a density contrast of 0.1 Mg m^{-3}. Contour interval 200 gu. (g) Magnitude of maximum horizontal gradient of the pseudogravity transform shown in (f). Contour interval 20 gu km^{-1}. (h) Locations of maxima of data shown in (g). Note correspondence with the actual edges of the source shown in (a). (Redrawn from Blakely & Connard 1989.)

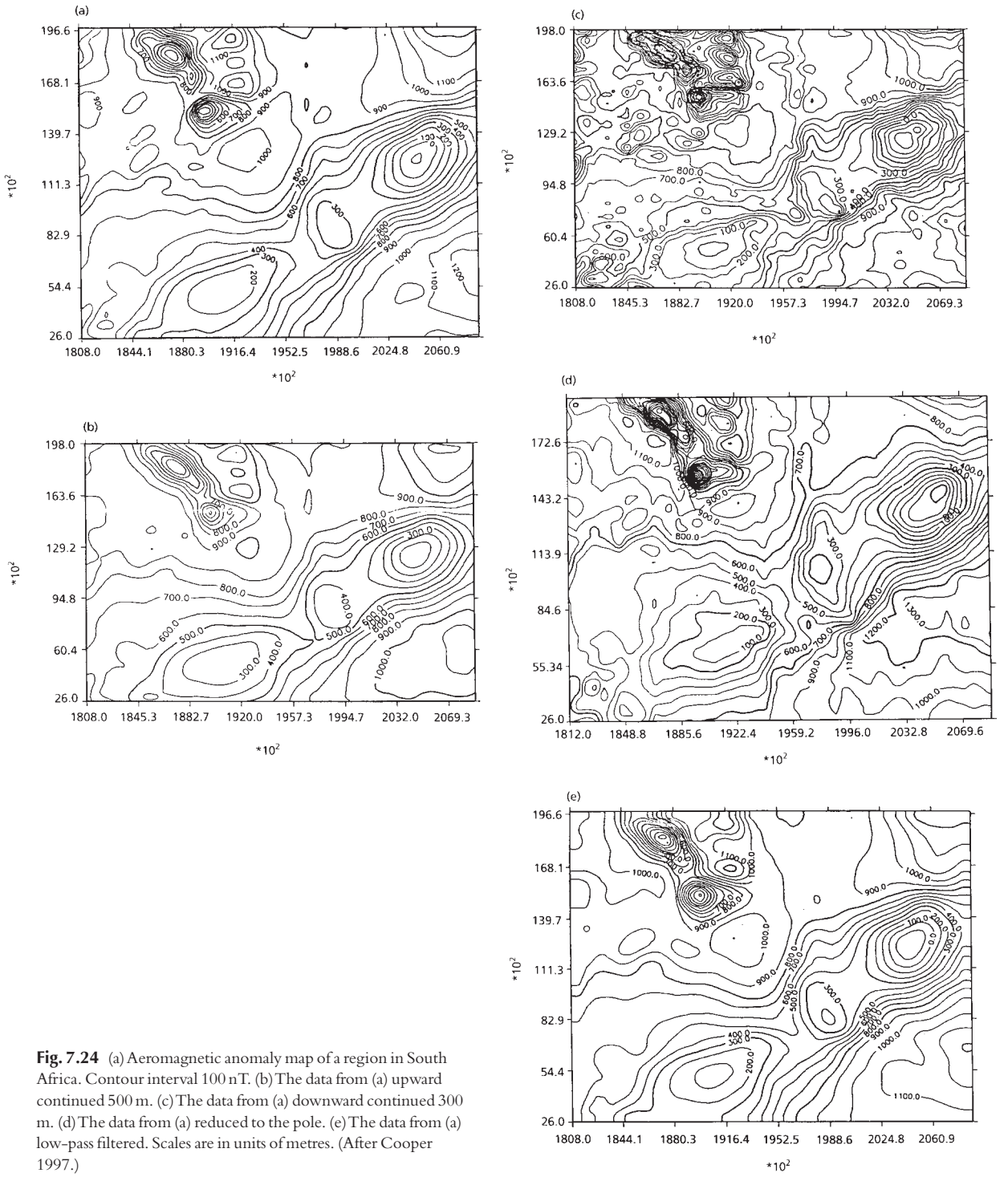

Fig. 7.24 (a) Aeromagnetic anomaly map of a region in South Africa. Contour interval 100 nT. (b) The data from (a) upward continued 500 m. (c) The data from (a) downward continued 300 m. (d) The data from (a) reduced to the pole. (e) The data from (a) low-pass filtered. Scales are in units of metres. (After Cooper 1997.)

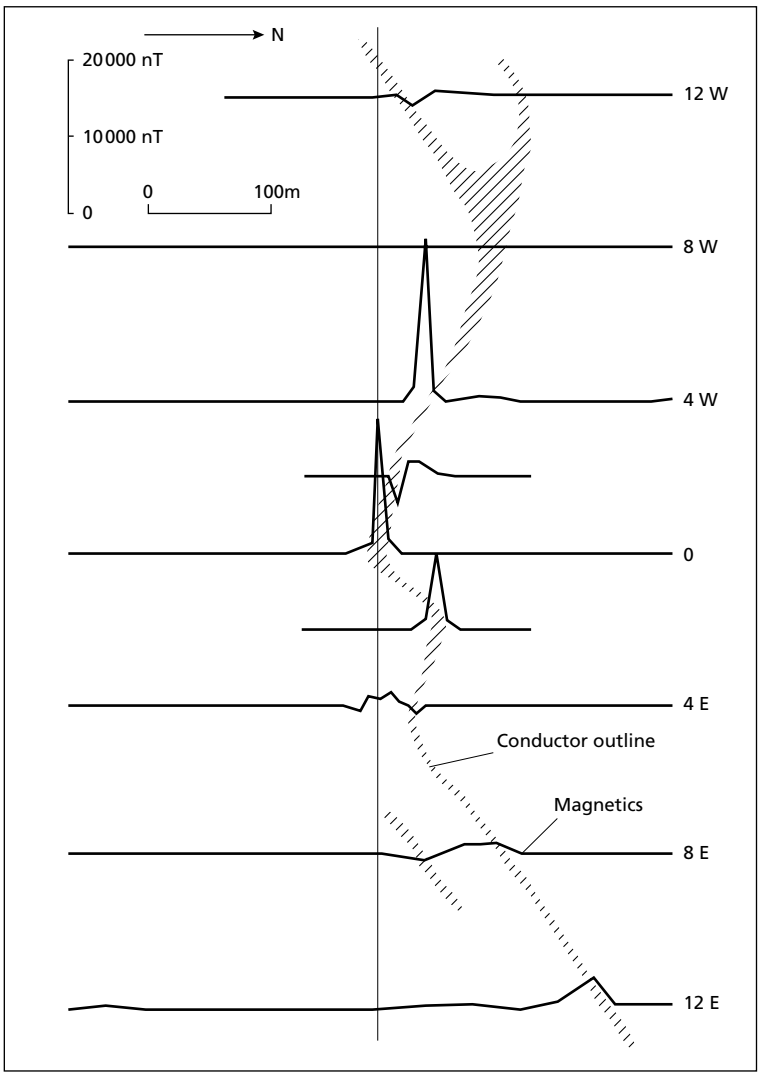

Fig. 7.25 Vertical field ground magnetic anomaly profiles over a massive sulphide ore body in Quebec, Canada. The shaded area represents the location of the ore body inferred from electromagnetic measurements. (After White 1966.)

In academic studies, magnetic surveys can be used in regional investigations of large-scale crustal features, although the sources of major magnetic anomalies tend to be restricted to rocks of basic or ultrabasic composition. Moreover, magnetic surveying is of limited use in the study of the deeper geology of the continental crust because the Curie isotherm for common ferrimagnetic minerals lies at a depth of about 20 km and the sources of major anomalies are consequently restricted to the upper part of the continental crust.

Although the contribution of magnetic surveying to knowledge of continental geology has been modest, magnetic surveying in oceanic areas has had a profound influence on the development of plate tectonic theory

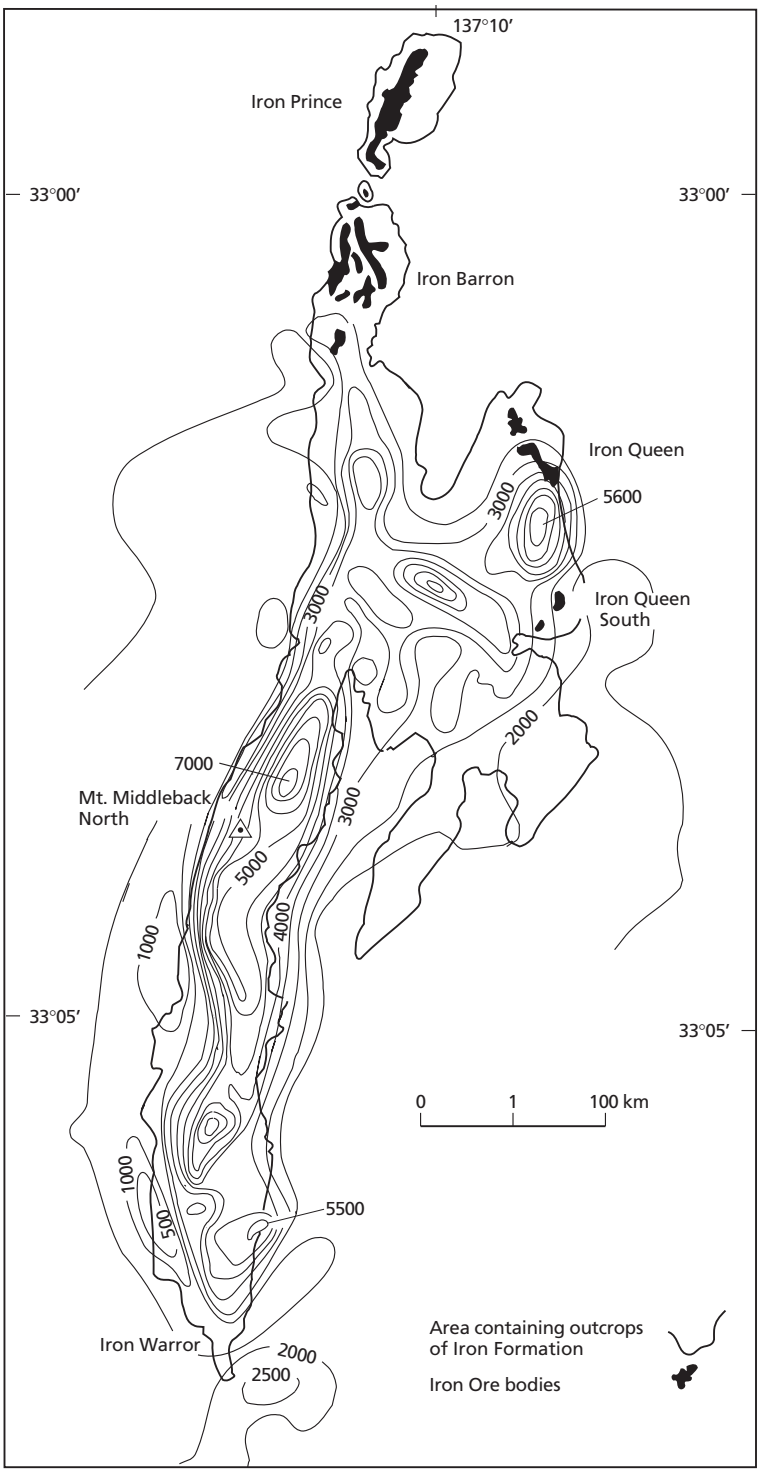

Fig. 7.26 Aeromagnetic anomalies over the Northern Middleback Range, South Australia. The iron ore bodies arc of haematite composition. Contour interval 500 nT. (After Webb 1966.)

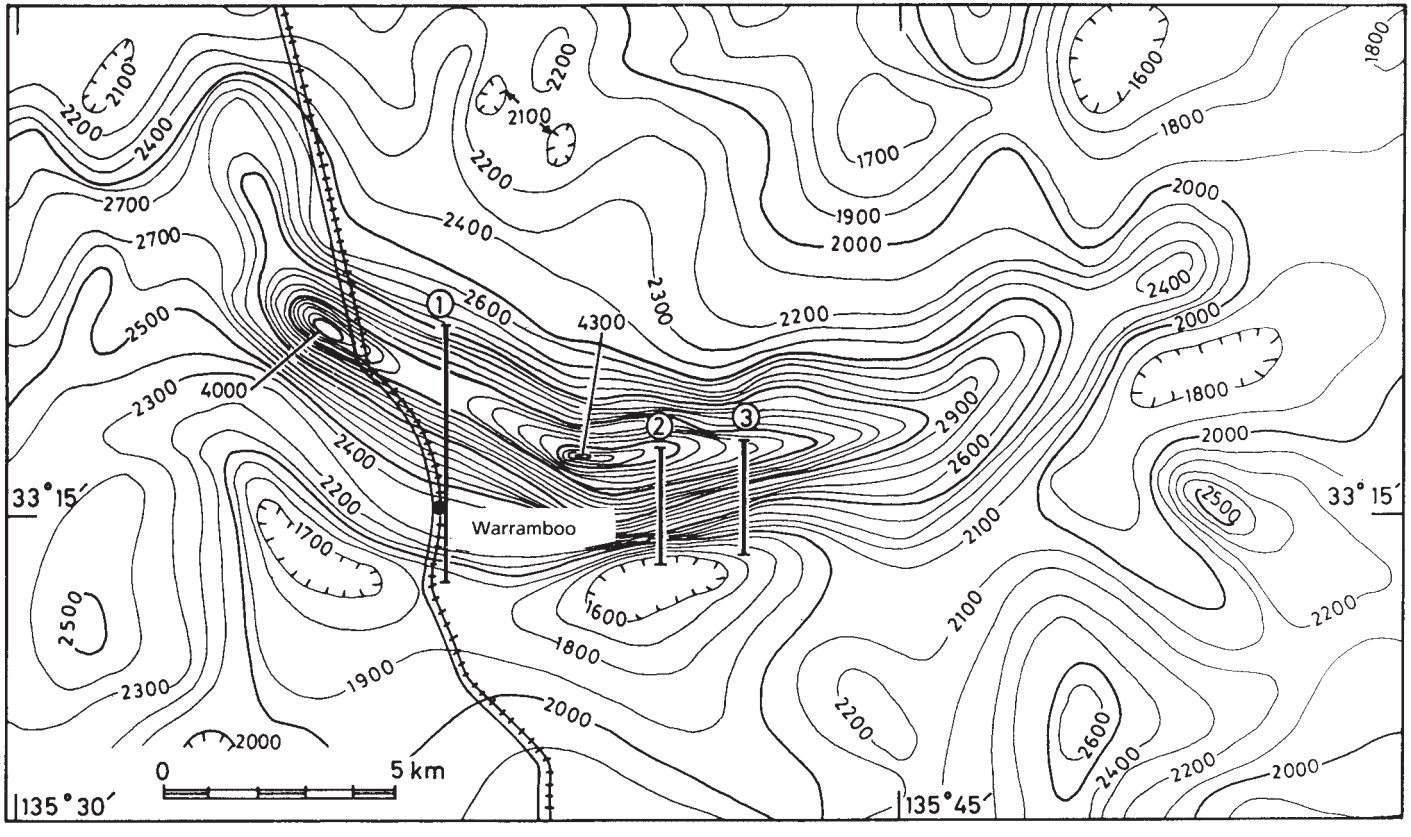

Fig. 7.27 High-level aeromagnetic anomalies over part of the Eyre Peninsula, South Australia. Contour interval 100 nT. (After Webb 1966.)

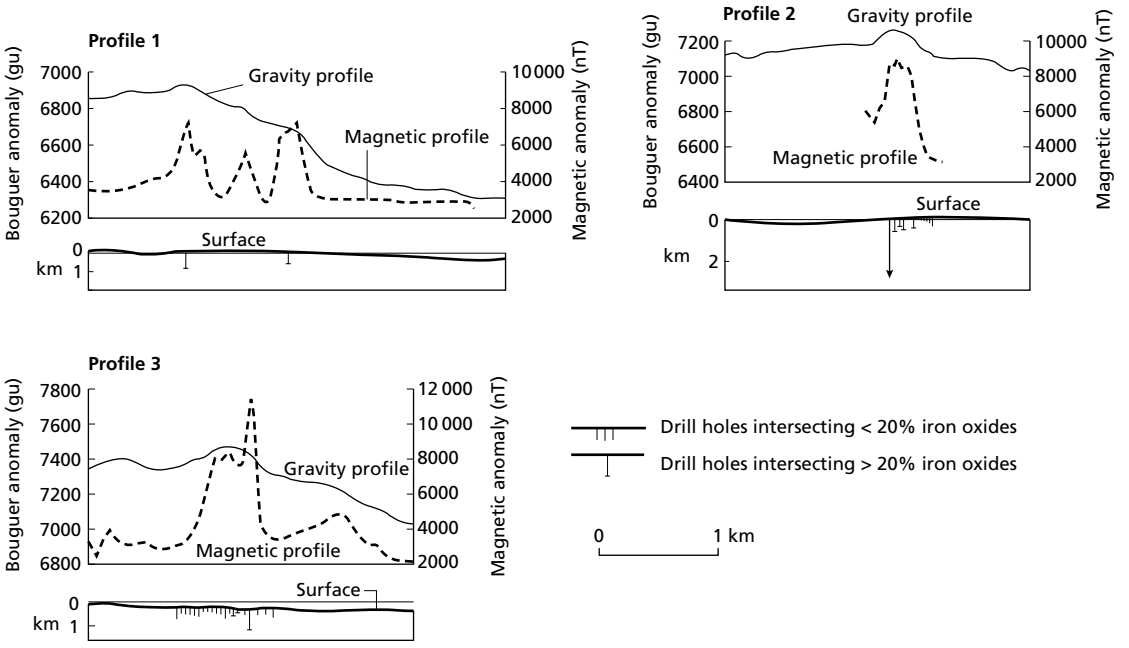

Fig. 7.28 Gravity and magnetic ground profiles over part of the Eyre Peninsula, South Australia, at the locations shown in Fig. 7.27 (After Webb 1966.)

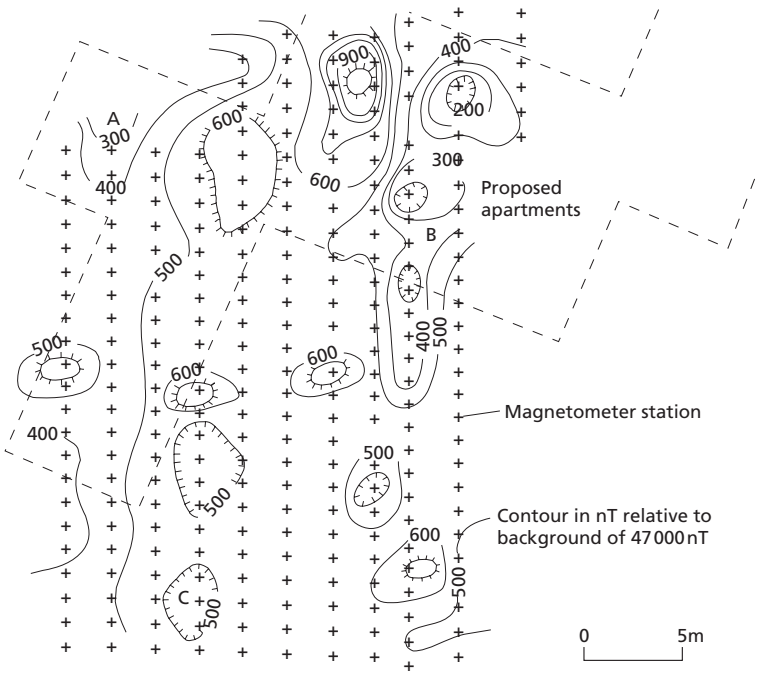

Fig. 7.29 Magnetic anomaly contour map of a site in Bristol, England. Contour interval 100 nT. (After Hooper & McDowell 1977.)

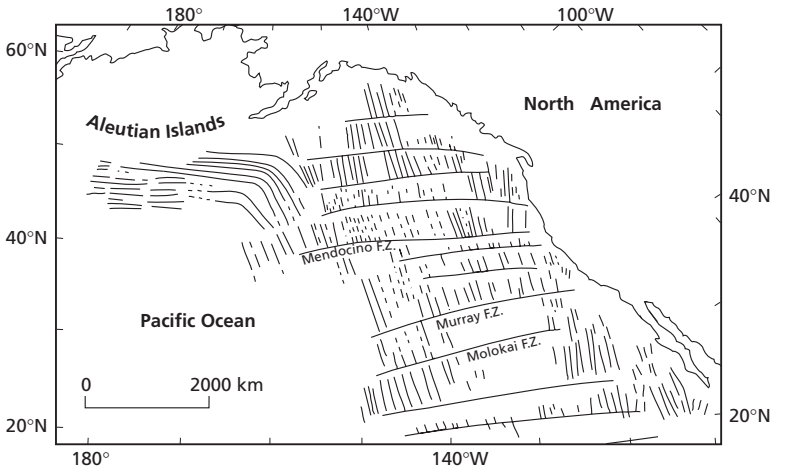

Fig. 7.30 Pattern of linear magnetic anomalies and major fracture zones in the northeast Pacific Ocean.

(Kearey & Vine 1996) and on views of the formation of oceanic lithosphere. Early magnetic surveying at sea showed that the oceanic crust is characterized by a pattern of linear magnetic anomalies (Fig. 7.30) attributable to strips of oceanic crust alternately magnetized in a normal and reverse direction (Mason & Raff 1961). The bilateral symmetry of these linear magnetic anomalies about oceanic ridges and rises (Vine & Matthews 1963) led directly to the theory of sea floor spreading and the establishment of a time scale for polarity transitions of the geomagnetic field (Heirtzler *et al.* 1968). Consequently, oceanic crust can be dated on the basis of the pattern of magnetic polarity transitions preserved in it.

Transform faults disrupt the pattern of linear magnetic anomalies (see Fig. 7.30) and their distribution can therefore be mapped magnetically. Since these faults lie along arcs of small circles to the prevailing pole of rotation at the time of transform fault movement, individual regimes of spreading during the evolution of an ocean basin can be identified by detailed magnetic surveying. Such studies have been carried out in all the major oceans and show the evolution of an ocean basin to be a complex process involving several discrete phases of spreading, each with a distinct pole of rotation.

Magnetic surveying is a very useful aid to geological mapping. Over extensive regions with a thick sedimentary cover, structural features may be revealed if magnetic horizons such as ferruginous sandstones and shales, tuffs and lava flows are present within the sedimentary sequence. In the absence of magnetic sediments, magnetic survey data can provide information on the nature and form of the crystalline basement. Both cases are applicable to petroleum exploration in the location of structural traps within sediments or features of basement topography which might influence the overlying sedimentary sequence. The magnetic method may also be used to assist a programme of reconnaissance geological mapping based on widely-spaced grid samples, since aeromagnetic anomalies can be employed to delineate geological boundaries between sampling points.

Problems

1. Discuss the advantages and disadvantages of aeromagnetic surveying.
2. How and why do the methods of reduction of gravity and magnetic data differ?
3. Compare and contrast the techniques of interpretation of gravity and magnetic anomalies.
4. Assuming the magnetic moment of the Earth is 8×10^{22} A m^2, its radius 6370 km and that its

Continued

magnetic field conforms to an axial dipole model, calculate the geomagnetic elements at 60°N and 75°S. Calculate also the total field magnetic gradients in $nT\,km^{-1}$ N at these latitudes.

5. Using equations (7.18a,b,c), derive expressions for the horizontal, vertical and total field magnetic anomalies of a vertical dyke of infinite depth striking at an angle α to magnetic north.

Given that geomagnetic inclination I is related to latitude θ by $\tan I = 2 \tan \theta$, use these formulae to calculate the magnetic anomalies of east–west striking dykes of width 40 m, depth 20 m and intensity of magnetization $2\,A\,m^{-1}$, at a latitude of 45°, in the following cases:

(a) In the northern hemisphere with induced magnetization.

(b) In the northern hemisphere with reversed magnetization.

(c) In the southern hemisphere with normal magnetization.

(d) In the southern hemisphere with reversed magnetization.

How would the anomalies change if the width and depth were increased to 400 m and 200 m, respectively?

6. (a) Calculate the vertical, horizontal and total field magnetic anomaly profiles across a dipole which strikes in the direction of the magnetic meridian and dips to the south at 30° with the negative pole at the northern end 5 m beneath the surface. The length of the dipole is 50 m and the strength of each pole is 300 A m. The local geomagnetic field dips to the north at 70°.

(b) What is the effect on the profiles if the dipole strikes 25°E of the magnetic meridian?

(c) If the anomalies calculated in (a) actually originate from a cylinder whose magnetic moment is the same as the dipole and whose diameter is 10 m, calculate the intensity of magnetization of the cylinder.

(d) Fig. 7.31 shows a total field magnetic anomaly profile across buried volcanic rocks to the south of Bristol, England. Does the profile constructed in (a) represent a reasonable simulation of this anomaly? If so, calculate the dimensions and intensity of magnetization of a possible magnetic source. What other information would be needed to provide a more detailed interpretation of the anomaly?

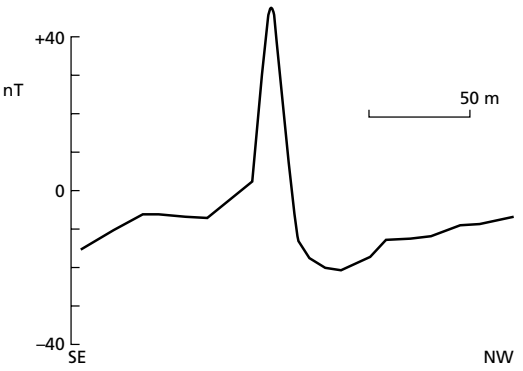

Fig. 7.31 Total field magnetic profile across buried volcanic rocks south of Bristol, England. (After Kearey & Allison 1980.)

Further reading

Arnaud Gerkens, J.C. d' (1989) *Foundations of Exploration Geophysics*. Elsevier, Amsterdam.

Baranov, W. (1975) *Potential Fields and Their Transformation in Applied Geophysics*. Gebrüder Borntraeger, Berlin.

Bott, M.H.P. (1973) Inverse methods in the interpretation of magnetic and gravity anomalies. *In*: Alder, B., Fernbach, S. & Bolt, B.A. (eds), *Methods in Computational Physics*, **13**, 133–62.

Garland, G.D. (1951) Combined analysis of gravity and magnetic anomalies *Geophysics*, **16**, 51–62.

Gibson, R.I. & Millegan, P.S. (eds) (1998) *Geologic Applications of Gravity and Magnetics: Case Histories*. SEG Reference Series 8 & AAPG Studies in Geology 43, Tulsa.

Gunn, P.J. (1975) Linear transformations of gravity and magnetic fields. *Geophys. Prosp.*, **23**, 300–12.

Kanasewich, E.R. & Agarwal, R.G. (1970) Analysis of combined gravity and magnetic fields in wave number domain. *J. Geophys. Res.*, **75**, 5702–12.

Nettleton, L.L. (1971) *Elementary Gravity and Magnetics for Geologists and Seismologists*. Monograph Series No. 1. Society of Exploration Geophysicists, Tulsa.

Nettleton, L.L. (1976) *Gravity and Magnetics in Oil Exploration*. McGraw-Hill, New York.

Sharma, P. (1976) *Geophysical Methods in Geology*. Elsevier, Amsterdam.

Stacey, F.D. & Banerjee, S.K. (1974) *The Physical Principles of Rock Magnetism*. Elsevier, Amsterdam.

Tarling, D.H. (1983) *Palaeomagnetism*. Chapman & Hall, London.

Vacquier, V., Steenland, N.C., Henderson, R.G. & Zeitz, I. (1951) Interpretation of aeromagnetic maps. *Geol. Soc. Am. Mem.*, **47**.